Rheol Acta
DOI 10.1007/s00397-016-0985-9

ORIGINAL CONTRIBUTION

Progress in numerical simulation of yield stress fluid flows

Pierre Saramito[1] · **Anthony Wachs**[2,3]

Received: 3 October 2016 / Accepted: 21 November 2016

Abstract Numerical simulations of viscoplastic fluid flows have provided a better understanding of fundamental properties of yield stress fluids in many applications relevant to natural and engineering sciences. In the first part of this paper, we review the classical numerical methods for the solution of the non-smooth viscoplastic mathematical models, highlight their advantages and drawbacks, and discuss more recent numerical methods that show promises for fast algorithms and accurate solutions. In the second part, we present and analyze a variety of applications and extensions involving viscoplastic flow simulations: yield slip at the wall, heat transfer, thixotropy, granular materials, and combining elasticity, with multiple phases and shallow flow approximations. We illustrate from a physical viewpoint how fascinating the corresponding rich phenomena pointed out by these simulations are.

Special Issue to celebrate the centennial anniversary of the seminal Bingham paper

✉ Pierre Saramito
Pierre.Saramito@imag.fr

1 Laboratory J. Kuntzmann, CNRS and Grenoble University, 38058 Grenoble cedex 9, France

2 Department of Mathematics, University of British Columbia, 1984 Mathematics Road, Vancouver, BC V6T 1Z2, Canada

3 Department of Chemical and Biological Engineering, University of British Columbia, 2360 East Mall, Vancouver, BC V6T 1Z3, Canada

Keywords Bingham viscosity · Computer modeling · Constitutitve equation · Modelling · Herschel-Bulkley · Yield stress

Introduction

The first model for fluids with plasticity has been introduced at the end of the nineteenth century by Schwedoff (1900) for gelatin suspensions. Schwedoff was the forerunner to a multitude of papers on variable viscosity effects in a plethora of materials which were to occupy much of the literature of the first half of the twentieth century. In their historical review, Tanner and Walters (1998, p. 26) pointed out that, during this period, "*there was a tendency to label all anomalous behavior as manifestations of 'plasticity', with no clear idea as to what that meant.*" The work of Bingham (1916, 1922) introduced some clarifications and provided a great deal of information on measurements for various systems, including gel-like materials with a yield stress. While this mathematical model was expressed for simple shear flow only, its extension to a general three-dimensional flow was introduced in 1947 by Oldroyd (1947), based on the von Mises criterion.

Numerically simulating the flow of a yield stress material is not a straightforward task. Assuming that rheological models with a threshold in terms of the norm of the deviatoric part of the stress tensor, i.e., a von Mises criterion, represent a satisfactory approximation of the observable behavior of a material, the mathematical non-smoothness of these models and the indeterminacy of the stress tensor below the yield stress threshold render the design of appropriate solution methods subtler than for a simple purely viscous material. Over the past 40 years, essentially two families of solution methods were suggested in the literature, the so-called regularization approach and augmented Lagrangian algorithm. The former solution method circumvents the aforementioned two problematic mathematical properties by simply modifying the constitutive equation such that it is smooth and well determined regardless of the shear rate magnitude, including zero. The latter solution method introduces two additional new tensorial fields and solves the whole problem as the minimization of a functional with a step descent Uzawa algorithm. While the regularization approach was very popular in the 1980s and 1990s, the community has been progressively acknowledging over the past 10 years that, although solving a slightly different problem (the regularized problem) might be fine in some flow configurations, it also leads to some questions about the relevance of the computed solution, in particular in terms of the location of *yield surfaces* and the modeling of the finite time decay property. While the augmented Lagrangian algorithm and its variants solve the actual yield stress model, their main drawback is their prohibitive computational cost related to a rather slow convergence rate. New active research directions over the second decade of the twenty-first century aim at developing algorithms for solving the initial, unregularized, problem but with a faster convergence rate and lower computing time. This will open up new perspectives in the numerical simulation of yield stress fluid flows; in particular, it might eventually make simulation of three-dimensional flows possible.

Section “Introduction” presents the viscoplastic flow problem and its mathematical statement. Section “Problem statement” reviews the two main algorithmic approaches: (i) regularization approach and (ii) augmented Lagrangian algorithm. This section closes by a review of recent strategies for fast-and-accurate algorithms. Section “Algorithms for viscoplastic models” presents common extensions of the conventional viscoplastic Bingham and Herschel-Bulkley models: yield slip at the wall, non-constant coefficients (granular materials, mixtures, thermal effects, or thixotropy), elasticity, and shallow flow-reduced models.

Problem statement

The total Cauchy stress tensor of a viscoplastic fluid is expressed by $\boldsymbol{\sigma}_{\text{tot}} = -p\,I + \boldsymbol{\sigma}$, where $\boldsymbol{\sigma}$ denotes its deviatoric part and p is the pressure. The constitutive equation for a viscoplastic fluid writes:

$$\begin{cases} \boldsymbol{\sigma} = 2K\,|2D(\boldsymbol{u})|^{n-1}D(\boldsymbol{u}) + \sigma_0 \frac{D(\boldsymbol{u})}{|D(\boldsymbol{u})|} & \text{if } |D(\boldsymbol{u})| \neq 0 \\ |\boldsymbol{\sigma}| \leq \sigma_0 & \text{if } |D(\boldsymbol{u})| = 0, \end{cases} \quad (1)$$

where $\sigma_0 \geq 0$ is the yield stress, $K > 0$ is the consistency, $n > 0$ is the power-law index, $\boldsymbol{u}$ is the velocity field, $D(\boldsymbol{u}) = (\nabla\boldsymbol{u} + \nabla\boldsymbol{u}^T)/2$ is the rate-of-deformation tensor, and, for any tensor $\tau = (\tau_{ij})$, the notation $|\tau|$ represents the following matrix norm:

$$|\tau| = \sqrt{\frac{\tau:\tau}{2}} = \left(\frac{1}{2}\sum_{ij}\tau_{ij}^2\right)^{\frac{1}{2}}.$$

The 1/2 factor under the square root is only a convenient convention: for a simple shear flow, $\dot{\gamma} = |2D(\boldsymbol{u})|$ coincides with the absolute value of the shear rate; otherwise, it would be counted twice. Note that when $\sigma_0 = 0$ and $n = 1$, the model (1) reduces to the classical viscous incompressible fluid. When $\sigma_0 \geq 0$ and $n = 1$, we obtain the tridimensional extension of the Bingham model, as formulated by Oldroyd (1947). In the general case $\sigma_0 \geq 0$ and $n > 0$, we obtain the tridimensional extension of the Herschel and Bulkley (1926) model. Note also that tacking the norm of Eq. 1 leads to a simple scalar relation, suitable for simple shear flows:

$$|\boldsymbol{\sigma}| = K\,\dot{\gamma}^n + \sigma_0.$$

The conservation of momentum expresses:

$$\rho\left(\frac{\partial\boldsymbol{u}}{\partial t} + (\boldsymbol{u}.\nabla)\boldsymbol{u}\right) - \mathbf{div}\,\boldsymbol{\sigma} + \nabla p = \boldsymbol{f}, \quad (2)$$

where $\boldsymbol{f}$ denotes the external forces (e.g., the gravity) and ρ is the constant density. Thus, the mass conservation leads to the following:

$$\operatorname{div}\boldsymbol{u} = 0. \quad (3)$$

The set of Eqs. 1–3 is closed by some appropriate initial and boundary conditions and the problem is complete.

Note that the viscoplastic fluid is characterized by the following property: the material starts to flow only if the applied forces exceed the yield stress σ_0. When $\sigma_0 > 0$, one can observe *unyielded regions* in the interior of the fluid, where $D(\boldsymbol{u}) = 0$, i.e., where the material behaves as a solid. When σ_0 increases, these unyielded regions develop.

The mathematical analysis of this problem is an ongoing work. Mosolov and Miasnikov (1965, 1966, 1967) considered a variational formulation of the problem for a Poiseuille flow with a general non-circular cross section and studied qualitative properties of it. Existence and uniqueness of the solution and the structure of the flow were investigated, especially the shape of yield surfaces. Duvaut and Lions (1976) also provided a theoretical analysis for Poiseuille flows and flows in a reservoir. These authors investigated existence, uniqueness, and regularity of the solution for steady and non-stationary flows. Existence and extra regularity results on the problem with Dirichlet boundary conditions for a driven cavity flow were also studied by Fuchs and

Seregin (1997, 1998) (see also Fuchs et al. 1996; Fuchs and Seregin 2000, chap. 3). The expected regularity of the solution of the Bingham problem is still an open question, but it seems unreasonable to hope for a high regularity: in specific cases, such as Poiseuille or Couette flows, the velocity is known to have a limited regularity across the yield surface, separating yielded and unyielded regions.

Algorithms for viscoplastic models

This section starts with an historical overview, followed by a review of the two main solution methods available in the literature: the regularization approach and the augmented Lagrangian algorithm. A review of other recent methods completes this section.

Overview

The first numerical resolution was performed by Fortin (1972) for a flow in a pipe with a square section, based on a non-linear relaxation method. The augmented Lagrangian algorithm has been introduced in 1969 by Hestenes (1969) and Powell (1969). During the 1970s, this algorithm became popular for solving optimization problems (see e.g., Rockafellar (1976)). Then, Glowinski (1980) and Fortin and Glowinski (1983) proposed to apply it to the solution of the linear Stokes problem and also to other non-linear problems, including Bingham fluid flows. Bercovier and Engelman (1980) proposed a regularization approach by introducing a viscosity function. Another viscosity function was next proposed by Papanastasiou (1987). During the 1980s and the 1990s, numerical computations for Bingham flow problems were dominated by the regularization approach, perhaps due to its simplicity, while the augmented Lagrangian algorithm did not supply yet convincing results for practical viscoplastic flow applications. Glowinski and Le Tallec (1989) revisited the augmented Lagrangian algorithm, using new optimization and convex analysis tools, such as subdifferential, but no evidence of the efficiency of this approach to viscoplasticity was showed, while regularization methods became more popular in the 1990s with the work of Mitsoulis et al. (1993) and Wilson and Taylor (1996). Then, Saramito and Roquet (2001) showed for the first time the efficiency of the augmented Lagrangian algorithm, especially when combined with an auto-adaptive mesh technique for capturing accurately yield surfaces, across which the solution looses some regularity (see also Roquet and Saramito 2003). In the 2000s, this approach became mature and a healthy competition developed between the regularization approach and the augmented Lagrangian algorithm. Vola et al. (2003) obtained results for a driven cavity flow with the augmented Lagrangian algorithm while Mitsoulis and Huilgol (2004) presented computations for an expansion flow with the regularization approach. In a series of papers, Frigaard and coworkers pointed out some drawbacks of the regularization approach (Moyers-Gonzalez and Frigaard 2004; Frigaard and Nouar 2005; Putz et al. 2009). Finally, the augmented Lagrangian algorithm became the most popular way to solve viscoplastic flow problems because of its accuracy (Muravleva et al. 2010; Dimakopoulos et al. 2013), despite the fact that the regularization approach runs in general faster. The `Rheolef` library, a free software developed by one of the authors of this review article and supporting both the augmented Lagrangian algorithm and an auto-adaptive mesh technique, is now widely used for various flow applications (Putz and Frigaard 2010; Roustaei and Frigaard 2013; Wachs and Frigaard 2016; Boujlel et al. 2016).

The regularization approach

The main idea of the regularization approach is to modify the problem in order to recover standard equations. Let $\varepsilon \geq 0$ and set

$$\boldsymbol{\sigma}_\varepsilon = 2\left(K|2D(\boldsymbol{u})|^{n-1} + \frac{\sigma_0}{\left(|2D(\boldsymbol{u})|^2 + \varepsilon^2\right)^{\frac{1}{2}}}\right)D(\boldsymbol{u}),$$

where ε is the regularization parameter. When $\varepsilon = 0$, we recover the previous constitutive equation when $D(\boldsymbol{u}) \neq 0$. When $\varepsilon > 0$, the previous relation is well defined, even when $D(\boldsymbol{u}) = 0$.

Next, let us define the following viscosity function, proposed by Bercovier and Engelman (1980):

$$\eta_\varepsilon(\xi) = K\xi^{\frac{n-1}{2}} + \frac{\sigma_0}{(\xi + \varepsilon^2)^{\frac{1}{2}}}, \ \forall \xi \in \mathbb{R}^+.$$

Others variants of the viscosity function has been proposed: see e.g., Papanastasiou (1987), de los Reyes and González Andrade (2013), and also Frigaard and Nouar (2005) for a review and comparison of them. With this notation, the previous relation writes:

$$\boldsymbol{\sigma}_\varepsilon = 2\eta_\varepsilon\left(|2D(\boldsymbol{u})|^2\right)D(\boldsymbol{u}), \tag{4}$$

when $\varepsilon > 0$, the fluid is a quasi-Newtonian one. By this way, there is no more division by zero when $D(\boldsymbol{u}) = 0$, and we know efficient algorithms to solve such quasi-Newtonian fluid flow problems (see e.g., Saramito 2016a, chap. 2). Figure 1 plots the stress and the viscosity function versus the shear rate. Replacing the expression (4) of the stress in Eq. 2, we obtain, together with Eq. 3, a variant of the incompressible Navier-Stokes equations with a non-constant viscosity: this problem can be easily implemented by using any existing softwares dedicated to the solution of the Navier-Stokes equations.

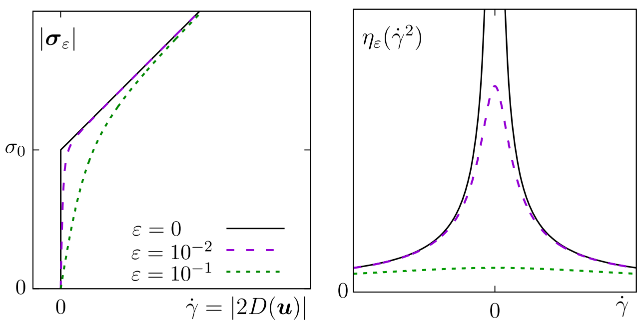

Fig. 1 Regularization for viscoplastic fluids: (*left*) the stress; (*right*) the viscosity

The simplest way to solve the nonlinear set of equations is the Picard fixed point method (see e.g., Abdali et al. 1992). For instance, combined with a Chorin pressure projection algorithm to deal with the incompressibility constraint and with a staggered finite difference discretization scheme, we obtain a popular approach, the so-called SIMPLE method, that is widely used in computational fluid dynamics and has been used for viscoplastic fluid flows by Syrakos et al. (2014). A more sophisticated way is the Newton method, that offers the advantage of a quadratic convergence rate of the residual terms. It was also investigated by several authors (Beverly and Tanner 1992; Smyrnaios and Tsamopoulos 2001; De los Reyes and González Andrade 2013; Aposporidis et al. 2011). These two nonlinear methods lead to a succession of linear system with a very bad condition number (the ratio of the largest eigenvalue to the smallest eigenvalue), due the large variations of the apparent viscosity η_ε. For bidimensional geometries or small to medium meshes, this linear system could be solved by a direct solver, while iterative solvers are required for large or tridimensional meshes. This last issue, and related preconditioning techniques, has been explored recently by Grinevich and Olshanskii (2009) and by Aposporidis et al. (2011, 2014).

A first weakness of the regularization approach is the lack of general convergence results of the solution with ε, denoted as $(\boldsymbol{\sigma}_\varepsilon, \boldsymbol{u}_\varepsilon)$ of the regularized problem to the original solution $(\boldsymbol{\sigma}, \boldsymbol{u})$ when $\varepsilon \longrightarrow 0$. Glowinski et al. (1981, p. 370) showed a convergence result for the velocity field $\boldsymbol{u}_\varepsilon$, in the case of the Bingham model ($n = 1$) and for the one-dimensional Poiseuille flow where the domain of computation Ω is a circular pipe section (see Zhang 2003 for some generalizations). There is no convergence results available concerning the corresponding stress deviator $\boldsymbol{\sigma}_\varepsilon$, and from numerical experiences, there is no evidence that this quantity converges to the solution $\boldsymbol{\sigma}$ associated to the unregularized problem (Frigaard and Nouar 2005; Putz et al. 2009): the velocity vector converged while decreasing ε whereas no convergence of the stress tensor is observed. Recall that the computation of the stress tensor is crucial for the determination of unyielded regions, characterized by $\{\boldsymbol{x} \in \Omega, \ |\boldsymbol{\sigma}_\varepsilon(\boldsymbol{x})| < \sigma_0\}$. Thus, we need a point-wise convergence of $\boldsymbol{\sigma}_\varepsilon$ to $\boldsymbol{\sigma}$ when ε tends to zero. Finally, regularized models may lead to an inaccurate prediction of unyielded regions. From Eq. 4, observe that $\boldsymbol{\sigma}_\varepsilon$ involves a product of η_ε and $D(\boldsymbol{u}_\varepsilon)$. There is an issue in unyielded regions, where the fluid is in rigid motion, i.e., where $D(\boldsymbol{u}_\varepsilon)$ tends to zero with ε. Recall that the velocity and its gradient are convergent with ε. In that case, as the viscosity η_ε involves a division by $|D(\boldsymbol{u}_\varepsilon)|$, this viscosity tends to infinity, their product in the expression of $\boldsymbol{\sigma}_\varepsilon$ appears as indeterminate, and there is no evidence that this product tends here to some finite value.

A second weakness of this approach is the disappearance of unyielded regions when tracked as $D(\boldsymbol{u}) = 0$. For instance, when solving the Poiseuille flow problem with this modified model, the velocity is not constant anymore at the center of the pipe. For the Couette flow, there is no motionless unyielded region anymore, and the position of the yielded surface is difficult to determine. Finally, with this modified problem, return to rest in finite time and *quiescent state* (Muravleva et al. 2010) cannot be captured: the flow never fully stops when the load is lower than the critical value. The finite time decay, quiescent state, and limit load analysis can not be established clearly. The prediction of stability of building foundations in civil engineering or mechanical robustness of engine parts becomes thus problematic. Also when trying to predict natural hazards, such as landslides, mud flows, snow avalanches, or volcanic lava flows, the disastrous event is always predicted, as the material can never be at the rest on a slope under gravity forces. Nevertheless, this approach remains simple to implement in existing codes (Mitsoulis et al. 1993; Tokpavi et al. 2008; Nikitin et al. 2011) and also useful when computations do not aim at predicting accurately either unyielded regions or a quiescent state. See also the review by Mitsoulis and Tsamopoulos (2016) in the present journal volume for some applications of the regularization approach. The next paragraph presents an alternative approach that is able to address accurately both unyielded regions and finite time decay to a quiescent state.

The augmented Lagrangian algorithm

In this paragraph, we consider a steady problem and the inertia term $(\boldsymbol{u}.\nabla)\boldsymbol{u}$ is also neglected. It is a common assumption, as many viscoplastic flows are slow. Here, this assumption is done without loss of generality: the inertia term can be reintroduced, e.g., as a right-hand side in a time-dependent algorithm, and at each time step, there is a stationary problem to solve, as considered in this paragraph. See e.g., Wachs et al. (2009) and Karimfazli et al.

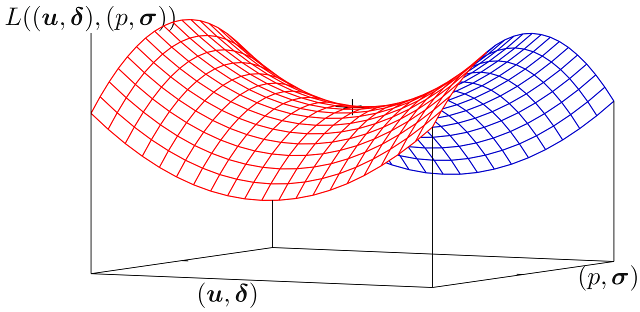

Fig. 2 Saddle-point problem formulation of a viscoplastic fluid flow

(2015) for such a simple explicit treatment of the inertia term, and Dean et al. (2007) and Muravleva (2015) for a more elaborated decoupled scheme.

The stationary and inertialess viscoplastic problem can be equivalently rewritten as the minimization of the viscous energy J defined by:

$$J(\boldsymbol{u}) = \int_\Omega \frac{K}{1+n} |2D(\boldsymbol{u})|^{1+n}\,\mathrm{d}x + \int_\Omega \sigma_0 |2D(\boldsymbol{u})|\,\mathrm{d}x - \int_\Omega \boldsymbol{f}.\boldsymbol{u}\,\mathrm{d}x$$

under the velocity divergence-free constraint and boundary conditions. Pressure represents as usual the Lagrange multiplier associated to the velocity divergence-free constraint. Here, a new independent variable $\boldsymbol{\delta}$, satisfying $\boldsymbol{\delta} = 2D(\boldsymbol{u})$, is introduced. The relation $\boldsymbol{\delta} = 2D(\boldsymbol{u})$ is treated as a new constraint and is imposed with a second Lagrange multiplier denoted as $\boldsymbol{\sigma}$. This notation is coherent, as $\boldsymbol{\sigma}$ coincides with the stress deviator. The situation is as follows:

constraint	Lagrange multiplier
$\mathrm{div}\ \boldsymbol{u} = 0$	p
$\boldsymbol{\delta} = 2D(\boldsymbol{u})$	$\boldsymbol{\sigma}$

The Lagrangian functional is defined by (see Fig. 2):

$$L\left((\boldsymbol{u},\boldsymbol{\delta}),\ (p,\boldsymbol{\sigma})\right) = \int_\Omega \frac{K}{1+n}|\boldsymbol{\delta}|^{1+n}\,\mathrm{d}x + \int_\Omega \sigma_0|\boldsymbol{\delta}|\,\mathrm{d}x - \int_\Omega \boldsymbol{f}.\boldsymbol{u}\,\mathrm{d}x - \int_\Omega p\,\mathrm{div}\,\boldsymbol{u}\,\mathrm{d}x + \frac{1}{2}\int_\Omega \boldsymbol{\sigma} : (2D(\boldsymbol{u}) - \boldsymbol{\delta})\,\mathrm{d}x + \frac{r}{2}\int_\Omega |2D(\boldsymbol{u}) - \boldsymbol{\delta}|^2\,\mathrm{d}x.$$

Here, $r \geq 0$ is an augmentation parameter, and when $r \neq 0$, the Lagrangian is called the augmented Lagrangian. Then, the corresponding saddle-point problem is equivalent to the previous minimization problem. It is solved by a specific constant step descent algorithm (Uzawa) with respect to the stress $\boldsymbol{\sigma}$: this is the so-called augmented Lagrangian algorithm. See e.g., Saramito (2016a, chap. 3) for a recent and detailed presentation of this algorithm.

There is mainly two methods in use for the discretization of the continuous problem: the finite element and the finite difference methods (see Fig. 3). Mixed finite elements were

Fig. 3 Some commonly used discretizations for the stress-velocity-pressure-mixed formulation. From top to bottom: $P_{1,\mathrm{disc}}$–P_2–P_1 and P_0–P_1–P_1 finite elements; staggered finite difference scheme

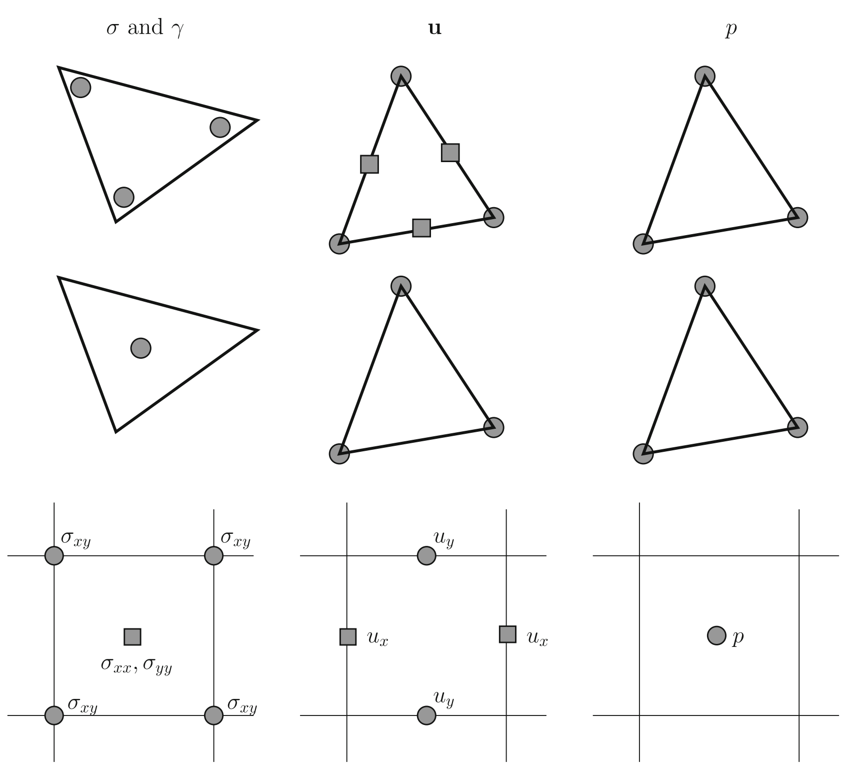

proposed by Roquet and Saramito (2003) with the Taylor-Hood P_2-P_1 approximation for the velocity-pressure pair and linear discontinuous approximation of the tensor variables (see also Roustaei and Frigaard 2013; Boujlel et al. 2016). Stabilized mixed finite elements was used by Vola et al. (2003) with the stabilized mini-element P_1-P_1 for the velocity-pressure pair and piecewise constant approximation of the tensor variables (see also Latché and Vola 2005; Zhang 2010). The finite difference method with staggered grids (sometimes called finite volume) was used by Vinay et al. (2005) (see also Muravleva et al. 2010; Glowinski and Wachs 2011; Karimfazli et al. 2015; Yu and Wachs 2007; Wachs et al. 2009): components of velocities and tensor components are not located at the same grid position, as shown on Fig. 3. Recently, Muravleva and Olshanskii (2008) explored a non-staggered finite difference scheme, where all velocity and stress components are located at the same grid position (see also Olshanskii 2009).

The first advantage of the augmented Lagrangian algorithm is its ability to compute an accurate prediction of yield surfaces, especially when combined with mesh adaptation (Saramito and Roquet 2001; Roquet and Saramito 2003; see also Fig. 4). This combination is now widely used for practical applications (Wachs 2007; Roustaei et al. 2015). Also, the quiescent state (limit load analysis) is well predicted (Saramito and Roquet 2001; Muravleva et al. 2010; Wachs and Frigaard 2016). The second advantage is that the algorithm reduces simply to a succession of Stokes-like subproblems with constant viscosity coefficients: these subproblems are easier to solve than the subproblems of the regularized approach, with very high viscosity variations.

The main drawback of the augmented Lagrangian algorithm is the computing time required to obtain the solution:

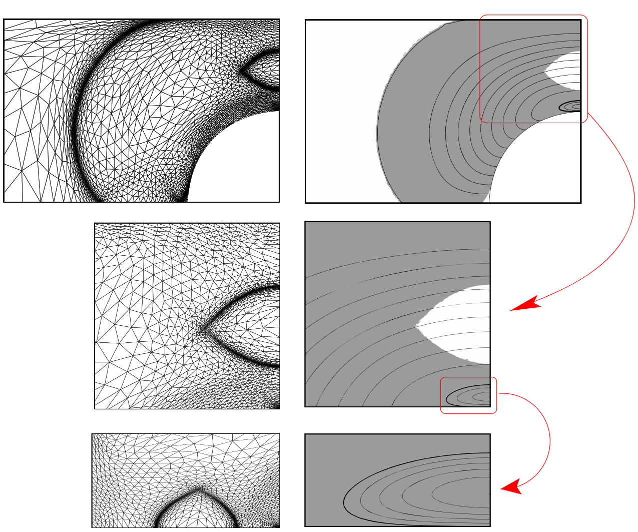

Fig. 4 Flow of a viscoplastic fluid around a moving cylinder: zoom on the adaptive mesh (from Roquet and Saramito 2003)

the next paragraph reviews some alternative approaches for solving more efficiently the unregularized viscoplastic problem.

Other unregularized approaches

While the regularization approach is relatively fast, at least when solved by a Newton algorithm, the accurate prediction of yielded surfaces could be problematic (Frigaard and Nouar 2005; Dimakopoulos et al. 2013). Conversely, the augmented Lagrangian algorithm is able to predict accurately the location of yield surfaces (Roquet and Saramito 2003) but its computing time is generally larger. Except the augmented Lagrangian algorithm, in the twentieth century, few unregularized approaches were known and were only valid for a very limited range of applications (Beris et al. 1985; Szabo and Hassager 1992). Recently, several attempts have been proposed to design *fast and accurate* algorithms for the resolution of the *unregularized* viscoplastic problem.

Recently, a semi-smooth Newton algorithm, combined with a Tikhonov regularization of the problem, was proposed by de los Reyes and González Andrade (2010, 2012). Nevertheless, a few years later (de los Reyes and González Andrade, 2013, p. 44), this approach has been found to be equivalent to a new variant of the regularization approach, as presented in "The regularization approach." The existence of commercial libraries dedicated to large optimization problems has been explored in 2015 by Bleyer et al. (2015). The authors claimed that their approach "*does not require any regularization of the viscoplastic model*," despite the fact that the used commercial library is based internally on an interior point method, i.e., a Newton method on a regularized problem combined with a continuation on the regularization parameter (see e.g., Boyd and Vandenberghe 2004, chap. 11). Finally, the point-wise convergence of the stress tensor and the related accuracy of unyielded regions predicted by this approach have not yet been addressed.

More recently, Aposporidis et al. (2014) proposed a Picard fixed point algorithm for a new reformulation of the unregularized viscoplastic problem. At each iteration, the linear system is solved by an iterative solver, and the solver is accelerated by an efficient preconditioning technique based on a regularization of the reformulated problem. Chupin and Dubois (2016) proposed a Chorin-like projection scheme combined with a Picard fixed point algorithm. Treskatis et al. (2016) explored an acceleration of the augmented Lagrangian algorithm based on the fast iterative shrinkage-thresholding algorithm (FISTA).

One of the most efficient algorithms to solve nonlinear problems is the Newton method, due to its super-linear convergence properties. Applying the Newton method to the unregularized viscoplastic problem leads to a singular

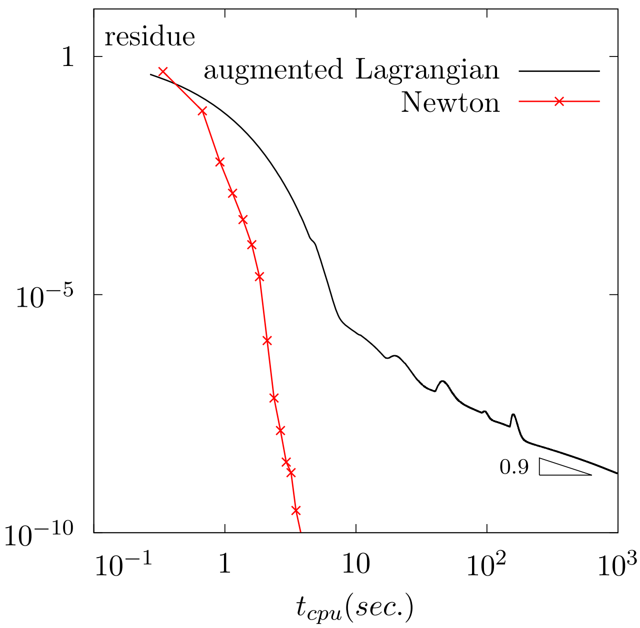

Fig. 5 Comparison between the Newton method and the augmented Lagrangian algorithm (AL) for the Herschel-Bulkley viscoplastic problem (from Saramito 2016b)

Jacobian matrix. This difficulty has been recently addressed by using the trusted region algorithm by Treskatis et al. (2015): the Jacobian matrix is regularized but the superlinear convergence of the method is lost. Saramito (2016b) addressed directly the singularity of the Jacobian matrix in the Newton method in order to preserve the superlinear convergence. Figure 5 plots the residue of the equations versus the computing time: observe the spectacular improvement of convergence for the solution of an unregularized viscoplastic problem.

Table 1 summarizes these various recent approaches and compares them in terms of their asymptotic convergence rate: there is actually three classes of algorithms for the unregularized problem. The more classical approach, the augmented Lagrangian, shows a polynomial convergence rate of the residual term $r_n \approx n^{-\alpha}$, where n is the iteration number and α is a constant. Plotting r versus n in log-log scale, as on Fig. 5, shows an asymptote with slope $\alpha \approx 0.9$. The FISTA acceleration (Treskatis et al. 2016) replaces α by 2α while the convergence remains polynomial. Both Picard fixed point (Aposporidis et al. 2014) and trust-region (Treskatis et al. 2015) methods improve this asymptotic convergence as $r_n = \exp(-\alpha n)$. The most efficient algorithm is certainly the Newton one (Saramito 2016b) with a quadratic convergence $r_n = \alpha\,(r_{n-1})^2$ (see also Fig. 5).

Extensions of the model

This section reviews various extensions of the conventional viscoplastic Bingham and Herschel-Bulkley models. Many viscoplastic fluids slips at the wall with a yield slip and corresponding slip models share some analogies with yield stress models (paragraph 3.1). Models with non-constant yield stress and consistency coefficients that depend on shear rate and pressure are commonly used for granular models (paragraph 3.2). Thixotropy (paragraph 3.3) supposes also a dependence of these coefficients on a material field; thermal effects (paragraph 3.4) introduce a dependence on temperature, while mixtures use a dependence on volume fraction (paragraph 3.5). Tacking into account the elasticity of the material leads to elastoviscoplastic models (paragraph 3.6). Finally, Shallow-flow approximations are commonly used for environmental and industrial applications when the vertical/horizontal aspect ratio of the flow is small (paragraph 3.7).

Yield slip boundary conditions

Slip occurs in the flow of two-phase systems, such as polymer solutions, emulsions, and particle suspensions, because of the displacement of the disperse phase away from solid boundaries. There is, close to the wall, a thin layer of fluid of lower viscosity than that of the bulk material, so that the shear amplitude is much larger in this layer than in the rest of the flow domain. This phenomenon appears to be more pronounced when the material possesses a yield stress, such as pastes. In practical viscoplastic flow problems such as concrete pumping, it also seems that a no-slip boundary condition is not a satisfactory model. The fluid slips when the tangential stress exceeds a critical value σ_s, called the yield

Table 1 What is fast and slow yield asymptotic convergence of various unregularized algorithms

Efficiency	Convergence	Rate	Methods and contributors
Slow	Power-law	$r_n = n^{-\alpha}$	Augmented Lagrangian (Roquet and Saramito 2003); FISTA (Treskatis et al. 2016)
Medium	Linear	$r_n = \exp(-\alpha n)$	Picard fixed point (Aposporidis et al. 2014) ; Trust-region (Treskatis et al. 2015)
Fast	Quadratic	$r_n = \alpha\,(r_{n-1})^2$	Newton (Saramito 2016b)

slip, and otherwise, the fluid sticks to the wall. This critical value may be considered as an intrinsic characteristic of the material and its relation to the wall. The slip boundary condition at the wall reads:

$$\begin{aligned} \boldsymbol{u}.\boldsymbol{n} &= 0 \\ \boldsymbol{\sigma}_{\boldsymbol{nt}} &= -c_f \boldsymbol{u_t} - \sigma_s \frac{\boldsymbol{u_t}}{|\boldsymbol{u_t}|} \quad \text{when } \boldsymbol{u_t} \neq 0 \\ |\boldsymbol{\sigma}_{\boldsymbol{nt}}| &\leq \sigma_s \quad\quad\quad\quad \text{when } \boldsymbol{u_t} = 0, \end{aligned}$$

where $\boldsymbol{u_t} = \boldsymbol{u} - \boldsymbol{u}.\boldsymbol{n}$ denotes the tangential velocity, $\boldsymbol{\sigma}_{\boldsymbol{nt}} = \boldsymbol{\sigma n} - \sigma_{\boldsymbol{nn}}.\boldsymbol{n}$ is the shear stress, $\sigma_{\boldsymbol{nn}} = (\boldsymbol{\sigma n}).\boldsymbol{n}$ the normal stress, $\boldsymbol{n}$ the outward unit normal at the wall, and $c_f > 0$ is a friction coefficient. We observe that for $\sigma_s = 0$, we obtain the classical linear slip boundary condition: the fluid slips for any non-vanishing shear stress. For $\sigma_s > 0$, boundary parts where the fluid sticks can be observed. As σ_s becomes larger, these stick regions develop.

Observe the analogy between the yield slip equation and the yield stress fluid constitutive (1). This analogy has been exploited by Fortin et al. (1991), who proposed an augmented Lagrangian algorithm for yield slip at the wall. Roquet and Saramito (2008) applied a similar approach to the Poiseuille flow of a viscoplastic fluid with a square cross section (see Fig. 6). Five flow regimes were identified in a master curve: full slip, full stick, partial slip and stick at the wall, block translation, and stopped material.

Damianou et al. (2014) investigated the time-dependent problem and the stopping time for a Poiseuille flow with a circular (Damianou et al. 2014) or square (Damianou et al. 2016) cross section with yield slip at the wall by using the regularization approach for both the viscoplastic model and the yield slip equation (Damianou and Georgiou 2014).

Models for dense granular material

Early concepts to explain the behavior of granular flows were introduced by Bagnold (1954), who identified many of the features of granular media. At the beginning of the twentieth century, from the collective work of the French research group *GDR milieux divisés* (Midi 2004; Jop et al. 2006), emerged for the first time a constitutive equation for the flow of dense dry granular materials, considered as a liquid. The deviatoric part $\boldsymbol{\sigma}$ of the Cauchy stress tensor is expressed by

$$\boldsymbol{\sigma} = 2\,\eta_{\text{app}}(p, |2D(\boldsymbol{u})|)\, D(\boldsymbol{u}),$$

where the apparent viscosity η_{app} depends on the pressure p and the shear rate $\dot\gamma = |2D(\boldsymbol{u})|$ as

$$\eta_{\text{app}}(p, \dot\gamma) = \frac{\mu(I)\,p}{\dot\gamma}, \quad \mu(I) = \frac{\mu_s I_0 + \mu_d I}{I_0 + I} \quad \text{and } I = \frac{d\,\dot\gamma}{\sqrt{p/\rho}}.$$

The inertial number I represents the square root of the Savage (1984) or Coulomb (Ancey et al. 1999) number while I_0 is a dimensionless number, d is the grain diameter and $\mu_d \geq \mu_s$ are frictions parameters for large and small I, respectively. This constitutive equation, often called $\mu(I)$-rheology, extended previous ideas introduced by Savage (1984), Savage and Hutter (1989), and Ancey et al. (1999). The $\mu(I)$-rheology was first used in numerical simulations in 2011 by Lagrée et al. (2011): these authors compared the solution with results of two-dimensional contact dynamics discrete simulations for the granular column collapse benchmark (see Fig. 7) and concluded that the constitutive equation is able to describe accurately the collapse for a large range of aspect ratios of the column. The unbounded apparent viscosity when $D(\boldsymbol{u})$ tends to zero was treated by bounding it numerically, and the whole system was solved by a Chorin's like decoupled projection algorithm. Chauchat and Médale (2010, 2013) proposed a regularization approach, inspired by those of Bercovier and Engelman (1980) for the Bingham model, and then solved the whole system by a Newton algorithm. Daviet and Bertails-Descoubes (2016), inspirated by Bleyer et al. (2015), used the interior point algorithm (i.e., a Newton method for a regularized problem combined with a continuation on the regularization parameter, see Boyd and Vandenberghe (2004, chap. 11) and our comments in "Other unregularized approaches"). Ionescu et al. (2015) addressed for the first time the unregularized $\mu(I)$ model and proposed an augmented Lagrangian algorithm, extending those presented by Roquet and Saramito (2003) for

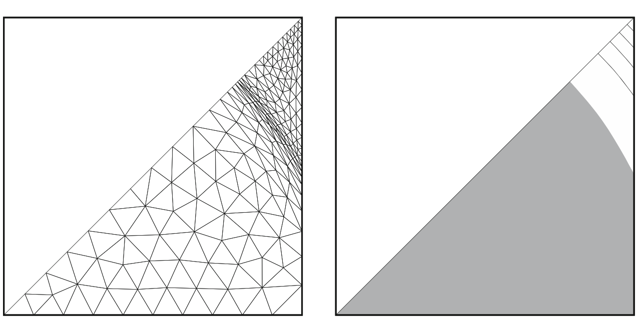

Fig. 6 Slip at the wall for a pipe flow of a Bingham fluid with a square section (from Roquet and Saramito 2008)

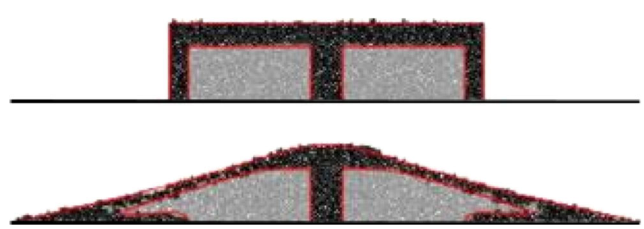

Fig. 7 Comparison between the $\mu(I)$ continuum model (*red line*) and contact dynamics simulations (*grains*) for a column collapse (initial and final state). The grains are colored in the initial heap, which allows one to track the displacement (from Lagrée et al. 2011)

the Bingham model. These authors observed that the $\mu(I)$-rheology coincides with an extension of the Bingham model (1) with non-constant viscosity and yield stress coefficients:

$$\begin{cases} \boldsymbol{\sigma} = 2\,\eta(p, |2D(\boldsymbol{u})|)D(\boldsymbol{u}) + \sigma_0(p)\frac{2D(\boldsymbol{u})}{|2D(\boldsymbol{u})|} & \text{if } |D(\boldsymbol{u})| \neq 0 \\ |\boldsymbol{\sigma}| \leq \sigma_0(p) & \text{if } |D(\boldsymbol{u})| = 0 \end{cases}$$

with

$$\sigma_0(p) = \mu_s p \text{ and } \eta(p, \dot{\gamma}) = \frac{(\mu_d - \mu_s)p}{\frac{I_0\sqrt{p}}{d\sqrt{\rho}} + \dot{\gamma}}.$$

Note that a simplified pressure-dependent (Coulomb-like) yield stress model is the Drucker and Prager (1952) model:

$$\sigma_0(p) = \overline{\sigma}_0 + \mu_s p \text{ and } \eta(p, \dot{\gamma}) = \overline{\eta}_0,$$

where $\overline{\sigma}_0$ and $\overline{\eta}_0$ are constants. Ionescu et al. (2015) found that the $\mu(I)$-rheology and Drucker-Prager models give very similar results for the granular column collapse benchmark. Simultaneously, Barker et al. (2015) showed that the $\mu(I)$ model could be mathematically ill-posed in some cases and then could develop Hadamard instabilities. These authors also proposed a well-posed variant (Barker et al. 2016):

$$\mu(I) = \frac{\mu_s I_0 + \mu_d I + \alpha I^2}{I_0 + I},$$

where $\alpha > 0$ is a stabilization parameter.

Thixotropy

The literature on thixotropic materials is extremely vast, but every thixotropic material is not necessarily a viscoplastic material, and some of them are purely viscous. Cement slurries, drilling muds, cosmetics and personal care products, waxy crude oils, and fire-fighting foams are among many examples of thixotropic viscoplastic materials. Viscoplasticity is often related to a particular micro-structure of the material: jamming, colloidal forces, soft chemical bonds, fiber orientation, etc. This micro-structure evolves over short times to breakdown when the material is subjected to a certain stress or strain load (Cheng 1986; Goddard 1984; Barnes 1997; Mujumdar et al. 2002; Coussot 2007; Ovarlez et al. 2010). Conversely, it evolves over long times to recovery when left to rest. This micro-structure is generally described by a scalar field, denoted λ, that indicates the level of structuring of the material (Houska 1981; De Souza Mendes 2011; De Souza Mendes and Thompson 2013). A zero value represents a fully broken down material, and a value of 1 or $+\infty$, depending on the model, represents a fully structured material. In the vast majority of models, the yield stress σ_0 is a function of the field λ and hence, evolves with time and stress or strain rate.

In the late 1950s, Moore (1959) suggested an unsteady advection-reaction equation for the structure field λ, that covers a wide range of thixotropic materials. Moore depicted the material micro-structure as composed of a number of links with the rheological behavior of the material a function of the number of links formed. Moore interpreted the structure field λ as the ratio of formed links to the total number of potential links. Hence, when $\lambda = 0$, all links are destroyed, and when $\lambda = 1$, all links are formed. In the popular Houska (1981) model (see also Derksen and Prashkant 2009; Wachs et al. 2009; Glowinski and Wachs 2011), the reaction term comprises a shear rate-dependent breakdown term and a recovery term:

$$\frac{\partial \lambda}{\partial t} + \mathbf{u}.\nabla\lambda = a(1 - \lambda) - b\lambda\dot{\gamma}^m,$$

where l takes its values in [0, 1] and $\dot{\gamma}$ is the generalized shear rate. Also, a, b, and m are the three experimentally measurable constants of the model. Note that a has the dimension of the inverse of time; thus, $1/a$ represents the time scale of recovery. In many models, recovery is associated to Brownian rearrangement of the micro-structure. Here, m is a power-law index. When $m = 1$, b represents the magnitude of shear-induced structure breakdown and is dimensionless. Other models, e.g., Dullaert and Mewis (2005, 2006), may include a shear-induced recovery but are conceptually very similar as far as the advection-reaction equation for the structure field is concerned. Following Moore, consistency and yield stress of the material are function of the structure field λ. For instance, Houska (1981) suggested a linear dependence as follows:

$$K = \bar{K}_0 + l\bar{K}_1 \text{ and } \sigma_0 = \bar{\sigma}_0 + l\bar{\sigma}_1,$$

where $\bar{K}_0$ and $\bar{\sigma}_0$ denote consistency and yield stress of the fully broken down material, respectively, and $\bar{K}_0 + \bar{K}_1$ and $\bar{\sigma}_0 + \bar{\sigma}_1$ denote consistency and yield stress of the fully recovered material, respectively. The Houska model contains thus seven parameters ($a, b, m, \bar{K}_0, \bar{K}_1, \bar{\sigma}_0$, and $\bar{\sigma}_1$) that are all measurable experimentally (Cawkwell and Charles 1989; Henaut and Brucy 2001).

Note that the main issue in solving a thixotropic viscoplastic flow problem arises from the two-way coupling of the momentum conservation equation and the constitutive equation via the λ equation: the momentum conservation with $\mathbf{u}$ depends on λ through K and σ_0, and λ depends on $\mathbf{u}$ through the advection term $\mathbf{u}.\nabla\lambda$ in the equation above. Wachs et al. (2009) solved this coupled time-dependent set of equations by a decoupled approach, where the reaction term is treated explicitly, i.e., at the previous time step. Each time step reduces to an explicit computation for λ and a stationary viscoplastic subproblem (see also Glowinski and Wachs 2011). When the micro-structural changes do not occur too fast, this approach allows large time steps; otherwise, the time step should be decreased as the scheme is conditionally stable. When solving the stationary viscoplastic subproblem with an augmented Lagrangian algorithm, it is conceivable to also update λ during iterations without loosing the usual robust convergence properties. Negrão et al. (2011) solved this coupling by a combination of semi-explicitness and Newton algorithm.

Among the various flow configurations of interest to the viscoplastic community, the start up flow of a thixotropic and viscoplastic material in a pipe has received a significant attention (see Sestak et al. 1987; Cawkwell and Charles 1987; Wachs et al. 2009; Glowinski and Wachs 2011; Negrão et al. 2011; Ahmadpour and Sadeghy 2014; and the references therein). In fact, it is representative of the industrial problem of restarting the flow of a waxy crude oil in a pipeline, a major and costly issue for oil and gas companies. Combined to additional weakly compressible effects, the flow exhibits different mechanisms to restart. In particular, compressibility combined to thixotropy enables the flow to restart and recover steady-flowing conditions for a pressure drop lower than the classical estimate derived from a simple force balance, a remarkable property. The ability to restart can hence be mapped in a compressibility number-thixotropy number space, as illustrated in Fig. 8 and explained in Wachs et al. (2009).

Thermal effects

Viscoplastic fluid flows with heat transfer lead to a rich variety of flow patterns and unconventional dynamics. From the early ages of viscoplastic fluid flows, researchers got interested in heat transfer for obvious practical reasons in

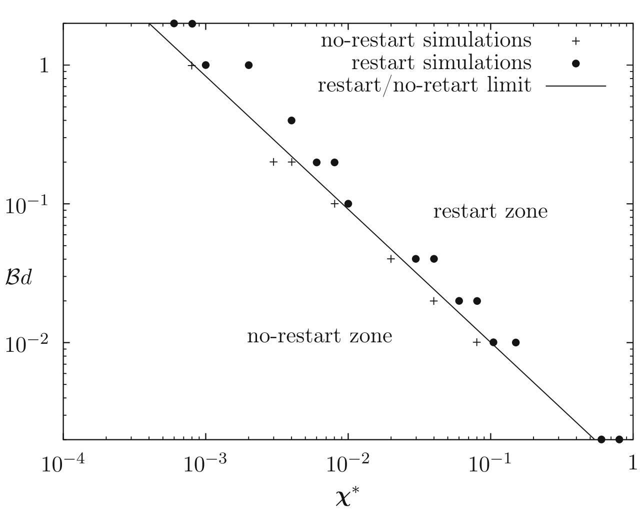

Fig. 8 Combined effects of thixotropy and compressibility for the restart of the weakly compressible flow in a pipeline filled with a viscoplastic and thixotropic material (from Wachs et al. 2009). The Bingham number is set to a value larger than the classical restart limit. χ^* and $\mathcal{B}d$ are dimensionless numbers for compressibility and thixotropy, respectively

industrial processes and flows. Some of the earliest references on an analytical work on heat transfer in Bingham fluid flows dates, to the best of our knowledge, from the late 1950s (Schechter and Wissler 1959; Yang and Yeh 1965; Duvaut and Lions 1972; Cherkasov 1979). Assuming the Boussinesq approximation $\rho = \rho_0(1 - \beta(\Theta - \Theta_r))$ holds, the most general non-isothermal viscoplastic fluid flow problems reads as follows:

$$\begin{aligned}
&\boldsymbol{\sigma} = 2K(\Theta)\,|2D(\boldsymbol{u})|^{n-1}\,D(\boldsymbol{u}) \\
&\qquad +\sigma_0(\Theta)\frac{2D(\boldsymbol{u})}{|2D(\boldsymbol{u})|} \qquad \text{if } |D(\boldsymbol{u})| \neq 0 \\
&|\boldsymbol{\sigma}| \leq \sigma_0(\Theta) \qquad \text{if } |D(\boldsymbol{u})| = 0 \\
&\rho_0 C_p \left(\frac{\partial \boldsymbol{\Theta}}{\partial t} + (\boldsymbol{u}.\nabla)\boldsymbol{\Theta}\right) - \mathbf{div}\, k\nabla\Theta - \boldsymbol{\sigma} : D(\boldsymbol{u}) = 0 \\
&\rho_0 \left(\frac{\partial \boldsymbol{u}}{\partial t} + (\boldsymbol{u}.\nabla)\boldsymbol{u}\right) - \mathbf{div}\,\boldsymbol{\sigma} + \nabla p = -\rho_0 \boldsymbol{g}\beta(\Theta - \Theta_r) \\
&\text{div}\,\boldsymbol{u} = 0
\end{aligned}$$

with suitable initial and boundary conditions. Here, Θ denotes the temperature field, ρ_0 the reference density at the reference temperature Θ_r, C_p the heat capacity, k the thermal conductibility, and β the thermal expansion coefficient at constant pressure.

Thermal effects as a result of significant temperature gradients manifest in a fluid flow with a growing level of complexity depending on the dependence or independence of material properties with temperature as follows:

(i) consistency K, yield stress σ_0, and density ρ are independent of temperature. The heat transfer regime is forced convection. The specificity of viscoplastic heat transfer stems from the convection term in the energy equation as the convecting velocity field is a viscoplastic velocity field. Momentum and energy conservation equations are one-way coupled only (Nirmalkar et al. 2013; Bose et al. 2014),

(ii) consistency K, yield stress σ_0, and density ρ are still independent of temperature but temperature gradients develop in the flow as a result of energy dissipation (Schechter and Wissler 1959). This is also referred to as *viscous heating* or heat generation. This situation has not received a large attention in the literature although it should lead to interesting temperature distribution. In fact, in a yield stress fluid flow, unyielded regions, by definition, do not dissipate energy, as $D(\boldsymbol{u}) = 0$ in these regions,

(iii) consistency K or yield stress σ_0 is temperature-dependent. The heat transfer regime is forced convection but now momentum and energy conservation equations are two-way coupled through the temperature dependence of the constitutive equation. In particular, the spatially variable yield stress as a function of temperature distribution can disturb the shape of yield surfaces (Vinay et al. 2005; Glowinski and Wachs 2011),

(iv) density ρ is temperature-dependent but this dependence is assumed to be weak such that the Boussinesq approximation is valid. The heat transfer regime is free (also called natural) convection over which an additional buoyancy term in the momentum equation drives motion (Zhang et al. 2006; Vikhansky 2009, 2010, 2011; Turan et al. 2010, 2011; Nirmalkar et al. 2014; Huilgol and Kefayati 2015; Karimfazli et al. 2015). Unsteady buoyancy-driven flows of a viscoplastic material can lead to a very unusual and remarkable intermittent behavior (Karimfazli et al. 2016).

In the aforementioned papers, a decoupled semi-explicit scheme is proposed for the time-dependent problem, i.e., at t^{n+1}:

1. solve the momentum equation with $\Theta^n = \Theta(t^n)$,
2. solve the energy equation with $\boldsymbol{u}^{n+1} = \boldsymbol{u}(t^{n+1})$.

Vinay et al. (2005) proposed a fully explicit loose-coupling scheme (see also Glowinski and Wachs 2011; Karimfazli et al. 2015, 2016) while Huilgol and Kefayati (2015) developed an operator splitting scheme. The resulting schemes are conditionally stable, and the time step should be chosen small enough for the scheme to converge accurately. Although this scheme is sufficient for most applications, it is possible to develop an unconditionally stable scheme. Turan et al. (2010, 2011) proposed a fully implicit time-dependent scheme with an inner fixed point loop. Note also that for computing the steady-state solution only, it is interesting to avoid a long-time evolution of a time-dependent problem. In that case, strongly coupled schemes with an inner loop of fixed-point or Newton methods are particularly well suited.

Two problems have received a broad attention from the community: (i) heat transfer from an obstacle in a viscoplastic fluid flow (Nirmalkar et al. 2013; Nirmalkar et al. 2014; Bose et al. 2014) and (ii) natural convection in a differentially heated cavity (Vikhansky 2009; 2010; 2011; Turan et al. 2010; Turan et al. 2011; Huilgol and Kefayati 2015; Karimfazli et al. 2015; 2016). The former problem is relatively simple and has been investigated mostly for steady-state flows with a regularization approach. It may however lead to intricate boundary layer problems and provides industrially valuable correlations of the Nüsselt number (dimensionless heat transfer coefficient) as a function of Reynolds and Bingham numbers. The latter problem is richer by essence and exhibits the usual unique features of a viscoplastic flow, i.e., existence of a critical Bingham B_{cr} for flow onset and finite time decay for Bingham number $B \leq B_{\mathrm{cr}}$. This problem has been investigated both with a regularization method (Vikhansky 2009, 2010, 2011; Turan et al. 2010, 2011) and with an augmented Lagrangian algorithm (Huilgol and Kefayati 2015; Karimfazli et al. 2015; 2016). These works all qualitatively agree with each other, although discrepancies exist in the definition and the value of B_{cr}. In a recent paper, Karimfazli et al. (2015) determined B_{cr} from augmented Lagrangian simulations and showed that this computed value matches the analytically derived conductive limit. They also proved finite time decay and unconditional stability of the static limit, both analytically and computationally. Slightly changing the boundary conditions of the problem by heating the bottom wall locally leads to intricate intermittencies called thermal plumes for specific ranges of B and other dimensionless numbers, observed both at the experimental level (Davaille et al. 2013) and at the simulation level (Karimfazli et al. 2016), and illustrated in Fig. 9.

Finally, very few simulation works investigated a temperature-dependent yield stress fluid flow problem and reported the effect of a spatially variable yield stress on the convergence of the selected solution algorithm (regularization or augmented Lagrangian). Figure 10 plots the convergence of the augmented Lagrangian algorithm as a function of the imposed temperature difference in the flow, which in turn indicates the amplitude of yield stress variations over the flow domain (Vinay et al. 2005). It is quite obvious that the convergence rate is markedly affected.

Two-phase flows

Many complex fluids also exhibit multiple phases, both in nature and in industry, e.g., bubbly flows, multi-layer flows, and particle-laden flows. Restricting the scope to two phases only, flows of interest can be classified into two families: (i) fluid/fluid flows either liquid/liquid or gas/liquid, and (ii) fluid/solid flows. Even if the fluid phase (respectively two fluid phases) is (respectively are) Newtonian, handling the co-existence of two phases in the flow requires a particular numerical treatment.

The most popular numerical modeling for fluid/fluid flows are arbitrary Lagrangian-Eulerian/mesh deforming methods (Fullsack 1995; Szabo and Hassager 1997; Alexandrou et al. 2003), volume-of-fluid (Hirt and Nichols 1981; Allouche et al. 2000; Hormozi et al. 2011; Tripathi et al. 2015; Liu et al. 2016), level set (Sussman et al. 1994; Singh and Denn 2008; Nikitin et al. 2011), or front tracking (Unverdi and Tryggvason 1992; Vola et al. 2004). For fluid/solid flows, there are arbitrary Lagrangian-Eulerian/mesh deforming methods (Fullsack 1995), lattice-Boltzmann (Ladd and Verberg 2001; Prashant 2011), immersed boundary (Mittal and Iaccarino 2005), and fictitious domain with distributed Lagrange multiplier (Yu and Wachs 2007; Wachs and Frigaard 2016).

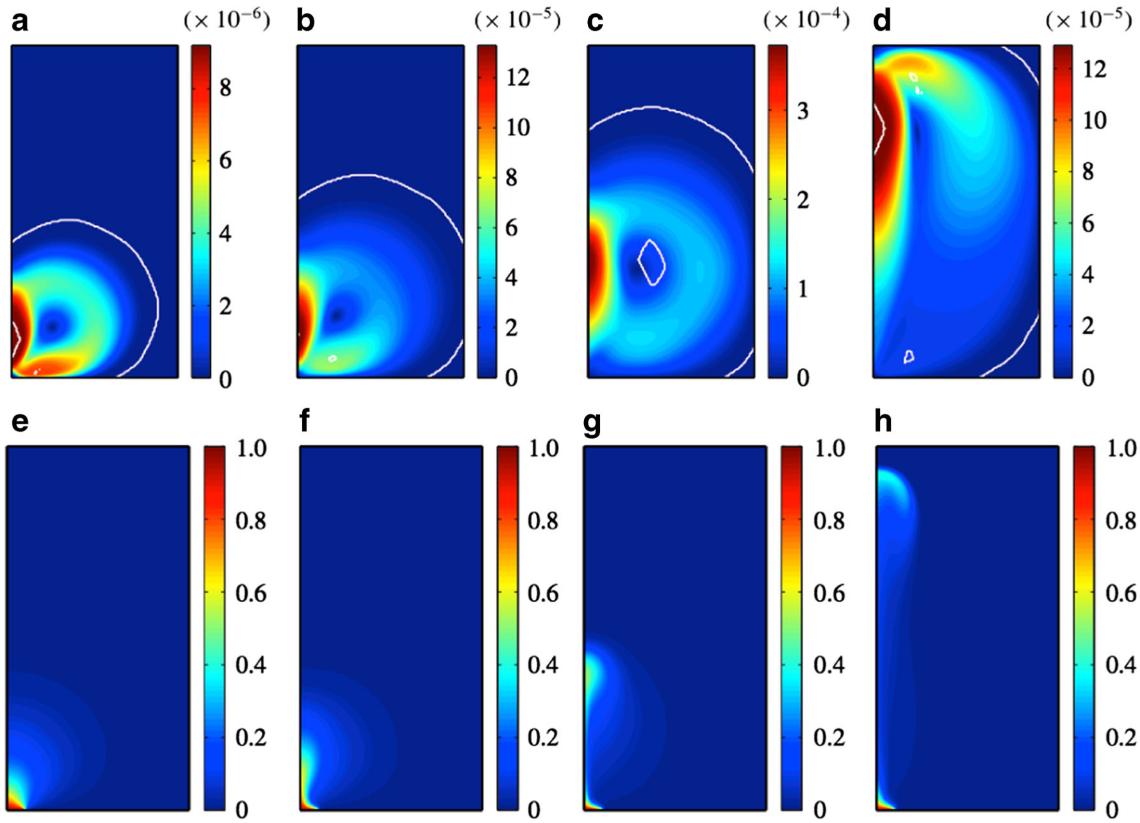

Fig. 9 Thermal plumes in a locally heated natural convection flow of a Bingham fluid in a cavity (from Karimfazli et al. 2016). **a–d** Time evolution of dimensionless velocity magnitude and yielded surface as a white line; **e–h** dimensionless temperature. Flow is heated from a narrow zone at the left of the bottom wall, left wall is a symmetry wall, and other walls are solid walls

Similarly to the case of thixotropy or thermal effects, semi-implicit and decoupled scheme are deemed to be sufficient to compute solutions of satisfactory accuracy for many applications. This is probably true for flow configurations with an imposed external motion but more questionable to compute finite time decay and limit of stationary flows. In the case of suspensions and emulsions, if a force balance has to be solved for the motion of each individual droplet, bubble, or particle, decoupled schemes might not be sufficient. In fact, in the case of a single rigid particle settling in a yield stress fluid, it has been recently emphasized by Wachs and Frigaard (2016) that a more sophisticated solution algorithm of the implicit or at least semi-implicit type is required to properly compute finite time decay and critical Bingham number beyond which motion is fully suppressed.

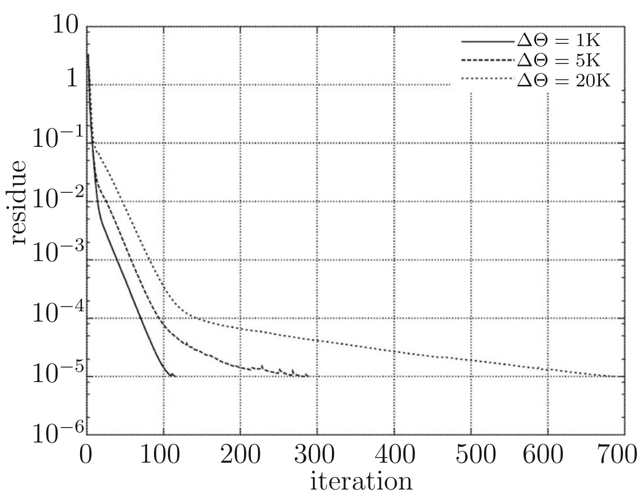

Fig. 10 Convergence of the augmented Lagrangian algorithm as a function of the imposed temperature difference $\Delta\Theta$ in the flow in a temperature-dependent yield stress fluid flow in a pipeline (from Vinay et al. 2005). The higher $\Delta\Theta$ is, the larger the amplitude of spatial variations of yield stress in the flow domain

Multi-layer and displacement flows have received a lot of attention in the literature in relation to their broad scope of applications in industry, e.g., well drilling and cement slurry placement in oil and gas (Szabo and Hassager 1997; Allouche et al. 2000; Hormozi et al. 2011) or molding in polymer processing (Dimakopoulos and Tsamopoulos 2003). Hormozi et al. (2011) investigate the stability of multi-layer viscoplastic channel flows and establish the stability properties of the flow. They are then capable of writing stable complex shapes of Newtonian fluid injected in a Bingham channel flow and advected along the channel. Note that these computations are performed with a decoupled scheme and a volume-of-fluid method.

A second class of problems that motivated various numerical works is free-surface flows as slumping flows (and in particular dam breaks, see also "Models for dense granular material") and extrusion flows. Slumping flows are model problems relevant to a large range of geophysical applications (Liu et al. 2016) as well as industrial processes (Vola et al. 2004; Alexandrou et al. 2003). In dam breaks, contrary to a Newtonian fluid that should theoretically slump infinitely if surface tension is neglected, viscoplastic materials stop at a finite run-out distance. This has important implications for hazard assessment (landslides and avalanches) and industrial safety (spill of a contaminated or dangerous fluid). For both (Vola et al. 2004) and Liu et al. (2016), a simple decoupled scheme is deemed to perform well. Figure 11 illustrates the original flow features unveiled by numerical simulations of Liu et al. (2016) of a slender slumping column made of a viscoplastic material.

The third class of problems that has been extensively studied over the past 20 years is the gravity-driven motion of dispersed droplet/bubble or solid particle in an otherwise quiescent yield stress fluid (Roquet and Saramito 2003; Nirmalkar et al. 2013; Nirmalkar et al. 2014; Bose et al. 2014; Singh and Denn 2008; Tsamopoulos et al. 2008; Prashant 2011; Dimakopoulos et al. 2013; Tripathi et al. 2015; Maleki et al. 2015; Wachs and Frigaard 2016). Actually, numerical works can be sorted into two sub-categories: (i) methods that really treat freely moving droplet/bubble or solid particle, and (ii) methods in which the problem is formulated in the droplet/bubble/particle frame of reference or as the flow past a motionless droplet/bubble/particle. Methods of the former sub-category can be applied to single droplet/bubble/particle flows or steady multi-droplet/bubble/particle flows while methods of the latter sub-category are more general. For instance, the flow past a fixed obstacle has been extensively studied as a model problem for suspension flows (Beaulne and Mitsoulis 1997; Blackery and Mitsoulis 1997; Zisis and Mitsoulis 2002; Roquet and Saramito 2003; Nirmalkar et al. 2013; Nirmalkar et al. 2014; Bose et al. 2014) and has provided some valuable insight into dimensionless drag and heat transfer coefficients and the shape of unyielded regions around the droplet/bubble/particle. The freely moving multi-droplet/bubble/particle problem has not been examined yet from a computational viewpoint, although novel results were recently published on the accurate modeling of finite time decay in the single-particle case (see Fig. 12). With the convergence rate of solution algorithms currently available to solve viscoplastic fluid flows (both regularization and augmented Lagrangian), the computing cost associated to the solution of a viscoplastic fluid flow with multiple freely moving droplets/bubbles/particles is yet too prohibitive, even on massively parallel supercomputers.

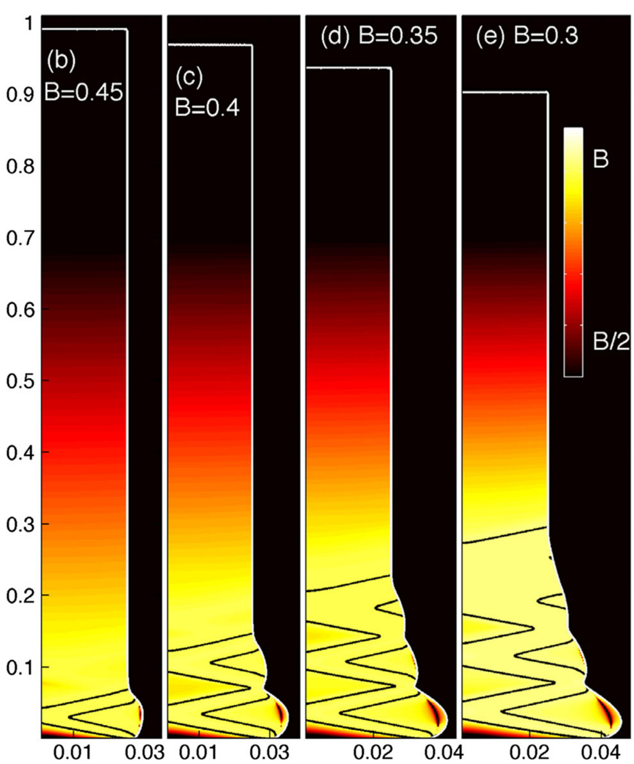

Fig. 11 Original flow features characterized by free-surface undulations and stress invariant zigzag pattern at the foot of a slender slumping column made of a viscoplastic material (from Liu et al. 2016)

Elastoviscoplastic models

The viscoplastic constitutive (1) writes equivalently (see e.g., Saramito 2007 or Saramito 2016a, chap. 5):

$$\max\left(0, \frac{|\boldsymbol{\sigma}| - \sigma_0}{K|\boldsymbol{\sigma}|^n}\right)^{\frac{1}{n}} \boldsymbol{\sigma} = 2D(\boldsymbol{u}).$$

Saramito (2007, 2009) proposed to take into account the elasticity of the material with a time-dependent constitutive equation:

$$\frac{1}{G}\overset{\square}{\boldsymbol{\sigma}} + \max\left(0, \frac{|\boldsymbol{\sigma}| - \sigma_0}{K|\boldsymbol{\sigma}|^n}\right)^{\frac{1}{n}} \boldsymbol{\sigma} = 2D(\boldsymbol{u}), \qquad (5)$$

where G is the elastic modulus and $\overset{\square}{\boldsymbol{\sigma}}$ denotes the Gordon and Schowalter (1972) derivative, which is a generalization of the frame-invariant Oldroyd (1950) derivative of the tensor $\boldsymbol{\sigma}$:

$$\overset{\square}{\boldsymbol{\sigma}} = \frac{\partial \boldsymbol{\sigma}}{\partial t} + (\boldsymbol{u}.\nabla)\boldsymbol{\sigma} - W(\boldsymbol{u})\boldsymbol{\sigma} + \boldsymbol{\sigma} W(\boldsymbol{u}) - a\left(D(\boldsymbol{u})\boldsymbol{\sigma} + \boldsymbol{\sigma} D(\boldsymbol{u})\right),$$

where $W(\boldsymbol{u}) = (\nabla \boldsymbol{u} - \nabla \boldsymbol{u}^T)/2$ is the vorticity tensor and $a \in [-1, 1]$ is a parameter of the derivative.

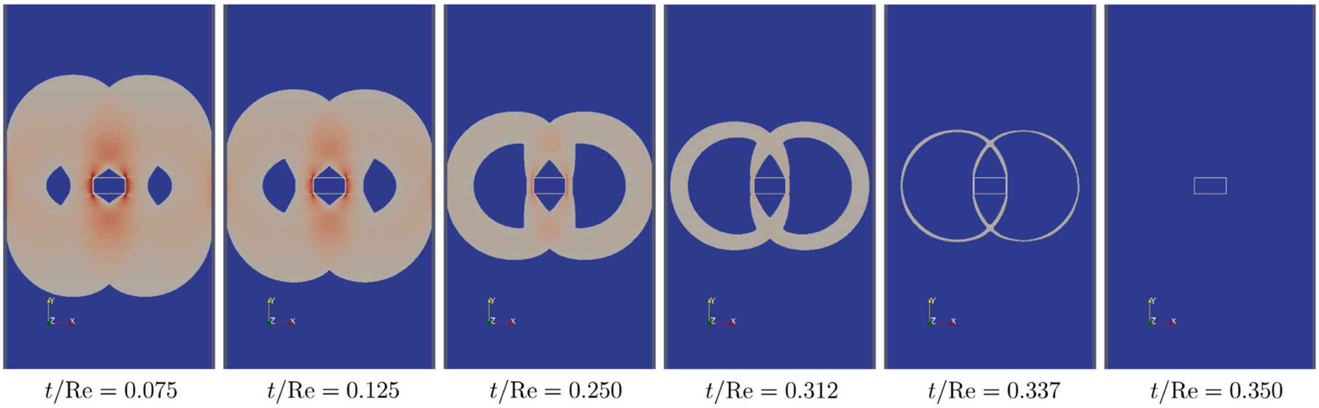

Fig. 12 Return to rest in finite time for a rectangular particle settling in a viscoplastic material (from Wachs and Frigaard 2016). The fluid/particle system has been initially assigned a Newtonian motion, and the yield stress increases abruptly from 0 to a value beyond the stationary limit. *Blue regions* are unyielded regions

This model has been first used for liquid foam by Cheddadi et al. (2008, 2012) for Couette flows and flows around a cylinder (Cheddadi et al. 2011). The set of equations is solved by a second order in time operator splitting scheme (Cheddadi and Saramito 2013), the so-called θ-scheme (Saramito 1994), previously developed for viscoelastic fluid flow problems. Figure 13 shows that there is very good *quantitative* agreement between calculations and experiments: the model captures quantitatively the fore-aft asymmetry and the overshoot of the velocity after the obstacle, located at $x = 0$. This overshoot of the velocity is often called the *negative wake*, in the context of a moving obstacle in a yield stress material at rest (i.e., u_x is then replaced by $-u_x$). Observe also on Fig. 13 that the Bingham model always predicts a fore-aft symmetry and no overshoot of the velocity: this is in disagreement with experimental observations on several yield stress materials

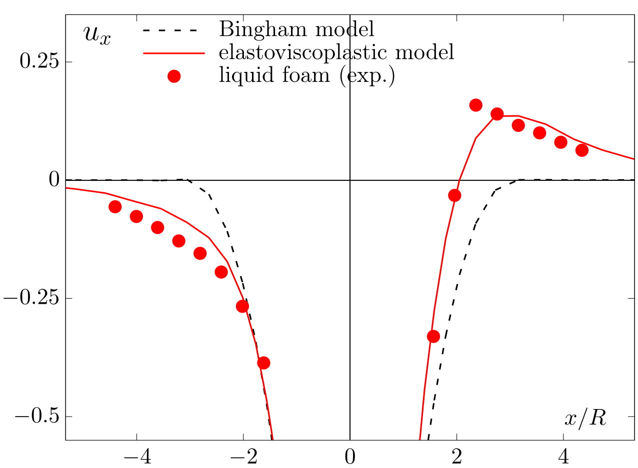

Fig. 13 Flow around a circular obstacle; velocity along the axis (from Cheddadi et al. 2011). Comparison between Bingham model (*dashed line*), elastoviscoplastic model (*solid line*), and liquid foam experiment (*closed squares*)

such as liquid foams and carbopol solutions. Fraggedakis et al. (2016) obtained a quantitative agreement between experiments with carbopol solutions around an obstacle and numerical simulations with the elastoviscoplastic model (5): loss of the fore-aft symmetry and formation of the negative wake.

In 2010, a regularized approach for solving the elastoviscoplastic model (5) was proposed by Park and Liu (2010), and results were compared to carbopol experiments for an oscillatory pipe flow. Comparisons between elastoviscoplastic model predictions and experiments in large amplitude oscillatory shear (LAOS) were performed by Ewoldt et al. (2010) and Dimitriou et al. (2013). Belblidia et al. (2011) also combined the elastoviscoplastic model (5) with a regularization approach and performed computations in a contraction-expansion geometry. De Souza Mendes (2011) combines both a regularized approach of viscoplasticity with elasticity and thixotropy (see also de Souza Mendes and Thompson 2013 and our "Thixotropy").

Shallow-flow approximations

Time-dependent three-dimensional simulations of free-surface flows are motivated by industrial and environmental applications, e.g., for the numerical prediction of many natural hazards, such as avalanches, landslides, volcanic lava, mud, or debris flows (see also "Models for dense granular material" and "Two-phase flows"). Generally, there is a large ratio between the two horizontal scales and the flow height, and this would require very large meshes. The development of reduced viscoplastic models for shallow flows is a less prohibitive computational cost approach: a three-dimensional problem reduces to a two-dimensional problem, and the free surface is directly handled by a height field that appears as an additional unknown in the reduced model.

For Newtonian fluids, this problem was first motivated by hydraulic engineering applications. Barré de Saint-Venant (1871) introduced the shallow water approximation for fast Newtonian flows, driven by inertia terms while viscous effects are neglected. More recently, Hupper (1982) investigated slower Newtonian flows and the effect of viscous terms heuristically, neglecting inertia terms, stating that the flow is locally one-dimensional and invoking the depth-integrated mass conservation equation, in order to get a nonlinear equation of the free-surface height. The technique has been revisited with the more general asymptotic expansion method: it leads to the same governing equation at zeroth expansion order, but provides a more general theoretical framework for the derivation of reduced models. But only the more complex non-Newtonian case approaches the complexity of both manufacturing processes (concretes, foods) and environmental applications. Concerning slow Bingham fluids, shallow-flow approximations were first studied by Liu and Mei (1990), based on a rigorous asymptotic expansion. The Liu and Mei approach was revisited by Balmforth and Craster (1999) and extended to the axisymmetric case (Balmforth et al. 2000), with application to volcanic lava domes. At the beginning of the twentieth century, this approach became mature: see Balmforth et al. (2006) and Ancey (2007) for some reviews on this subject during this period. Since 2010, many new ideas were developed in several directions: let us review them.

For granular materials, and based on an heuristic derivation, Savage and Hutter (1989) developed reduced models. These ideas were revisited by Gray and Edwards (2014) with a depth-averaged version of the $\mu(I)$-rheology. Fernández-Nieto ED et al. (2016) extended this shallow model as a multi-layer model (Audusse and Bristeau 2007) that allows to compute three-dimensional profiles of the velocity in the directions along and normal to the slope.

For fast flows, such as debris and mud flows on mountain slopes, Laigle and Coussot (1997) derived the first reduced model that combines both inertia and viscoplastic effects (see also Rickenmann et al. 2006). Viscoplastic effects are estimated from the friction at the bottom. Assuming a compressible material, Bresch et al. (2009) derived a reduced viscoplastic model that also includes inertia effects, and the set of equations was solved by an augmented Lagrangian algorithm (see also Acary-Robert et al. 2012). This approach was next revisited in the incompressible case in terms of asymptotic analysis (Fernández-Nieto et al. 2010; 2012). Finally, Ionescu (2010) proposed an augmented Lagrangian algorithm for the shallow incompressible viscoplastic model with inertia terms.

While most computations were performed on uniform slopes, practical predictions of natural hazard require to take into account general tridimensional and complex topographies (see e.g., Bernabeu et al. 2014). A new approach for topography in shallow flow models was proposed by Bouchut et al. (2003); it relaxes most restrictions, such as slowly varying topographies (small curvatures, see also Bouchut and Westdickenberg 2004). Next, Ionescu (2013), considering Bingham and Drucker-Prager models, extended this approach with an elegant formulation based on surface differential operators (surface gradient and divergence) and also included inertia effects (see also Ionescu and Lupaşcu 2015). Finally, Fernández-Nieto et al. (2014) studied well-balanced schemes with wet or dry fronts for a viscoplastic model with both topography and inertia effects.

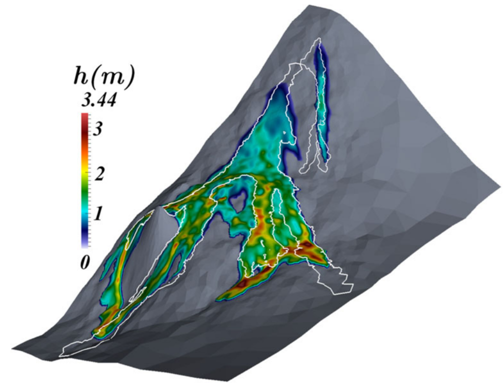

Fig. 14 Shallow-flow simulation of the volcanic lava flow predicted flow final deposit represented over the topography, with a color map showing the flow height h (from Bernabeu et al. 2016). The contour of the observed deposit zone provided by the Volcano Observatory of Piton de la Fournaise is represented by a *thin white line*

Shallow viscoplastic models with thermal coupling was studied by Balmforth et al. (2004) for lava domes and by Bernabeu et al. (2016) for lava flows on complex tridimensional topographies (see Fig. 14).

Conclusion

Viscoplastic models are widely used in science and engineering to investigate the flow dynamics of fluids with a yield stress. We have presented an extremely large variety of simulation results: many flow geometries, with slip at the wall, with heat transfer, with thixotropy, with elasticity, with multiple phases, and for shallow flows. The corresponding rich phenomena observed in these flows are fascinating from a physical viewpoint.

From the simple Bingham model to the most advanced extensions that include temperature dependence, thixotropy, or elasticity below the yield stress, the main challenge in numerical simulation remains the treatment of the non-smoothness of the Bingham or Herschel-Bulkley viscoplastic constitutive equation. Hence, the current research direction still pertains to developing new algorithms for the solution of the viscoplastic flow problem with a smaller computational cost while maintaining an accurate description of yield surfaces, at least as accurate as those provided by the augmented Lagrangian algorithm. The revival of augmented Lagrangian methods over the past 10 years and the progressive recognition that they are more accurate than regularization have created a new interest of the viscoplastic community to compute more reliable viscoplastic flow solutions. A simple multi-dimensional Bingham flow problem is a perfect toy problem to test the new family of unregularized approaches that has been recently suggested in the literature: FISTA, Picard fixed point, and Newton methods. These different methods all show promises for accelerated convergence, at least for flows in a simple geometry. The next step is now to examine how they perform in more complex geometries and if they can be even further accelerated.

Computational scientists interested in viscoplastic fluid flow simulations call for faster solution algorithms that preserve the accurate resolution of yield surfaces that the classical augmented Lagrangian method guarantees. Combined to new advances in high performance computing on large supercomputers, the milestone of three-dimensional numerical simulation of viscoplastic fluid flows as a standard should be attainable in the next few years.

References

Abdali SS, Mitsoulis E, Markatos NC (1992) Entry and exit flows of Bingham fluids. J Rheol 36(2):389–407

Acary-Robert C, Fernández-Nieto ED, Narbona-Reina G, Vigneaux P (2012) A well-balanced finite volume-augmented Lagrangian method for an integrated Herschel-Bulkley model. J Sci Comput 53(3):608–641

Ahmadpour A, Sadeghy K (2014) Start-up flows of Dullaert–Mewis viscoplastic–thixoelastic fluids: a two-dimensional analysis. J Non-Newt Fluid Mech 214:1–17

Alexandrou AN, Le Menn P, Georgiou GC, Entov V (2003) Flow instabilities of Herschel–Bulkley fluids. J Non-Newt Fluid Mech 116(1):19–32

Allouche M, Frigaard IA, Sona G (2000) Static wall layers in the displacement of two visco-plastic fluids in a plane channel. J Fluid Mech 424:243–277

Ancey C (2007) Plasticity and geophysical flows: a review. J Non-Newt Fluid Mech 142:4–35

Ancey C, Coussot P, Evesque P (1999) A theoretical framework for granular suspensions in a steady simple shear flow. J Rheol 43(6):1673–1699

Aposporidis A, Haber E, Olshanskii MA, Veneziani A (2011) A mixed formulation of the Bingham fluid flow problem: analysis and numerical solution. Comput Meth Appl Mech Engrg 200:2434–2446

Aposporidis A, Vassilevski PS, Veneziani A (2014) Multigrid preconditioning of the non-regularized augmented Bingham fluid problem. Elect Trans Numer Anal 41:42–61

Audusse E, Bristeau MO (2007) Finite-volume solvers for a multilayer Saint-Venant system. Int J Appl Math Comput Sci 17(3):311–320

Bagnold RA (1954) Experiments on a gravity-free dispersion of large solid spheres in a Newtonian fluid under shear. Proc R Soc Lond A 225:49–63

Balmforth NJ, Burbidge AS, Craster RV, Salzig J, Shen A (2000) Visco-plastic models of isothermal lava domes. J Fluid Mech 403:37–65

Balmforth NJ, Craster RV (1999) A consistent thin-layer theory for Bingham plastics. J Non-Newt Fluid Mech 84(1):65–81

Balmforth NJ, Craster RV, Rust AC, Sassi R (2006) Viscoplastic flow over an inclined surface. J Non-Newt Fluid Mech 139:103–127

Balmforth NJ, Craster RV, Sassi R (2004) Dynamics of cooling viscoplastic domes. J Fluid Mech 499:149–182

Barker T, Schaeffer DG, Bohorquez P, Gray JMNT (2015) Well-posed and ill-posed behaviour of the $\mu(I)$-rheology for granular flows. J Fluid Mech 779:794–818

Barker T, Schaeffer DG, Bohorquez P, Gray JMNT, Barker J (2016) Well-posed continuum modelling of granular flow. In: International Congress of Theoretical and Applied Mechanics

Barnes HA (1997) Thixotropy—a review. J Non-Newt Fluid Mech 70(1):1–33

Beaulne M, Mitsoulis E (1997) Creeping motion of a sphere in tubes filled with Herschel-Bulkley fluids. J Non-Newt Fluid Mech 72:55–71

Belblidia F, Tamaddon-Jahromi H, Webster M, Walters K (2011). Computations with viscoplastic and viscoelastoplastic fluids. Rheol Acta to appear

Bercovier M, Engelman M (1980) A finite-element method for incompressible non-Newtonian flows. J Comput Phys 36:313–326

Beris AN, Armstrong RC, Tsamopoulos J, Brown RA (1985) Creeping motion of a sphere through a Bingham plastic. J Fluid Mech 158:219–244

Bernabeu N, Saramito P, Smutek C (2014) Numerical modeling of shallow non-Newtonian flows: part II. Viscoplastic fluids and general tridimensional topographies. Int J Numer Anal Model 11(1):213–228

Bernabeu N, Saramito P, Smutek C (2016) Modelling lava flow advance using a shallow-depth approximation for three-dimensional cooling of viscoplastic flows. chap. 27. Geological Society, London

Beverly CR, Tanner RI (1992) Numerical analysis of three-dimensional Bingham plastic flow. J Non-Newt Fluid Mech 42(1):85–115

Bingham EC (1916) An investigation of the laws of plastic flow. Bul Bur Stand 13:309–353. https://archive.org/details/inv133093531916278278unse

Bingham EC (1922) Fluidity and plasticity. Mc Graw-Hill. New-York, USA. http://www.archive.org/download/fluidityandplast007721mbp/fluidityandplast007721mbp.pdf

Blackery J, Mitsoulis E (1997) Creeping motion of a sphere in tubes filled with a Bingham plastic material. J Non-Newt Fluid Mech 70(1):59–77

Bleyer J, Maillard M, De Buhan P, Coussot P (2015) Efficient numerical computations of yield stress fluid flows using second-order cone programming. Comput Meth Appl Mech Engrg 283:599–614

Bose A, Nirmalkar N, Chhabra RP (2014) Forced convection from a heated equilateral triangular cylinder in Bingham plastic fluids. Numer Heat Transf A 66(1):107–129

Bouchut F, Mangeney-Castelnau A, Perthame B, Vilotte JP (2003) A new model of Saint Venant and Savage-Hutter type for gravity driven shallow water flows. C R Math 336(6):531–536

Bouchut F, Westdickenberg M (2004) Gravity driven shallow water models for arbitrary topography. Comm Math Sci 2(3):359–389

Boujlel J, Pigeonneau F, Gouillart E, Jop P (2016) Rate of chaotic mixing in localized flows. Phys Rev Fluids 1(3):031301

Boyd SP, Vandenberghe L (2004) Convex optimization. Cambridge University Press, UK

Bresch D, Fernández-Nieto ED, Ionescu IR, Vigneaux P (2009) Augmented Lagrangian method and compressible visco-plastic flows:

applications to shallow dense avalanches. In: New directions in mathematical fluid mechanics. Springer, pp 57–89

Cawkwell MG, Charles ME (1987) An improved model for start-up of pipelines containing gelled crude-oil. J Pipelines 7(1):41–52

Cawkwell MG, Charles ME (1989) Characterization of Canadian Arctic thixotropic gelled crude oils utilizing an eight-parameter model. J Pipelines 7:251–264

Chauchat J, Médale M (2010) A three-dimensional numerical model for incompressible two-phase flow of a granular bed submitted to a laminar shearing flow. Comput Meth Appl Mech Engrg 199:439–449

Chauchat J, Médale M (2013) A three-dimensional numerical model for dense granular flows based on the $\mu(I)$ rheology. J Comput Phys 0. to appear

Cheddadi I, Saramito P (2013) A new operator splitting algorithm for elastoviscoplastic flow problems. J Non-Newt Fluid Mech 202:13–21

Cheddadi I, Saramito P, Dollet B, Raufaste C, Graner F (2011) Understanding and predicting viscous, elastic, plastic flows. Eur Phys J E 34(1):11001

Cheddadi I, Saramito P, Graner F (2012) Steady Couette flows of elastoviscoplastic fluids are non-unique. J Rheol 56(1):213–239

Cheddadi I, Saramito P, Raufaste C, Marmottant P, Graner F (2008) Numerical modelling of foam Couette flows. Eur Phys J E 27(2):123–133

Cheng DC (1986) Yield stress: a time-dependent property and how to measure it. Rheol Acta 25(5):542–554

Cherkasov SG (1979) Combined convection of a viscoplastic liquid in a plane vertical layer. Fluid Dyn 14(6):901–903

Chupin L, Dubois T (2016). A bi-projection method for Bingham type flows. submitted https://hal.archives-ouvertes.fr/hal-01166406

Coussot P (2007) Rheophysics of pastes: a review of microscopic modelling approaches. Soft Matter 3(5):528–540

Damianou Y, Georgiou GC (2014) Viscoplastic Poiseuille flow in a rectangular duct with wall slip. J Non-Newt Fluid Mech

Damianou Y, Kaoullas G, Georgiou GC (2016) Cessation of viscoplastic Poiseuille flow in a square duct with wall slip. J Non-Newt Fluid Mech 233:13–26

Damianou Y, Philippou M, Kaoullas G, Georgiou GC (2014) Cessation of viscoplastic Poiseuille flow with wall slip. J Non-Newt Fluid Mech 203:24–37

Davaille A, Gueslin B, Massmeyer A, Di Giuseppe E (2013) Thermal instabilities in a yield stress fluid: existence and morphology. J Non-Newt Fluid Mech 193:144–153

Daviet G, Bertails-Descoubes F (2016) Nonsmooth simulation of dense granular flows with pressure-dependent yield stress. J Non-Newt Fluid Mech 234:15–35

Dean EJ, Glowinski R, Guidoboni G (2007) On the numerical simulation of Bingham visco-plastic flow: old and new results. J Non-Newt Fluid Mech 142:36–62

Derksen JJ (2009) Simulations of complex flow of thixotropic liquids. J Non-Newt Fluid Mech 160(2):65–75

De los Reyes JC, González Andrade SA (2010) Numerical simulation of two-dimensional Bingham fluid flow by semismooth Newton methods. J Comput Appl Math 235:11–32

De los Reyes JC, González Andrade SA (2012) A combined BDF-semismooth Newton approach for time-dependent Bingham flow. Numer Meth Part Diff Eqn 28(3):834–860

De los Reyes JC, González Andrade SA (2013) Numerical simulation of thermally convective viscoplastic fluids by semismooth second order type methods. J Non-Newt Fluid Mech 193:43–48

De Souza Mendes PR (2011) Thixotropic elasto-viscoplastic model for structured fluids. Soft Matter 7(6):2471–2483

De Souza Mendes PR, Thompson RL (2013) A unified approach to model elasto-viscoplastic thixotropic yield-stress materials and apparent yield-stress fluids. Rheol Acta 52:673–694

Dimakopoulos Y, Pavlidis M, Tsamopoulos J (2013) Steady bubble rise in Herschel–Bulkley fluids and comparison of predictions via the augmented Lagrangian method with those via the Papanastasiou model. J Non-Newt Fluid Mech 200:34–51

Dimakopoulos Y, Tsamopoulos J (2003) Transient displacement of a viscoplastic material by air in straight and suddenly constricted tubes. J Non-Newt Fluid Mech 112(1):43–75

Dimitriou CJ, Ewoldt RH, McKinley GH (2013) Describing and prescribing the constitutive response of yield stress fluids using large amplitude oscillatory shear stress (Laostress). J Rheol 57(1):27–70

Drucker DC, Prager W (1952) Soil mechanics and plastic analysis of limit design. Q Appl Math 10:157–175

Dullaert K, Mewis J (2005) Thixotropy: build-up and breakdown curves during flow. J Rheol 49(6):1213–1230

Dullaert K, Mewis J (2006) A structural kinetics model for thixotropy. J Non-Newt Fluid Mech 139(1):21–30

Duvaut G, Lions JL (1972) Transfert de chaleur dans un fluide de Bingham dont la viscosité dépend de la température. J Func Anal 11(1):93–110

Duvaut G, Lions JL (1976) Inequalities in mechanics and physics. Springer

Ewoldt RH, Winter P, Maxey J, McKinley GH (2010) Large amplitude oscillatory shear of pseudoplastic and elastoviscoplastic materials. Rheol Acta 49(2):191–212

Fernández-Nieto ED, Gallardo JM, Vigneaux P (2014) Efficient numerical schemes for viscoplastic avalanches. Part 1: the 1D case. J Comput Phys 264:55–90

Fernández-Nieto ED, Garres-Díaz J, Mangeney A, Narbona-Reina G (2016) A multilayer shallow model for dry granular flows with the $\mu(I)$ rheology: application to granular collapse on erodible beds. submitted

Fernández-Nieto ED, Noble P, Vila JP (2010) Shallow water equations for non-Newtonian fluids. J Non-Newt Fluid Mech 165(13):712–732

Fernández-Nieto ED, Noble P, Vila JP (2012) Shallow water equations for power law and Bingham fluids. Sci China Math 55(2):277–283

Fortin A, Côté D, Tanguy PA (1991) On the imposition of friction boundary conditions for the numerical simulation of Bingham fluid flows. Comput Meth Appl Mech Engrg 88(1):97–109

Fortin M (1972) Calcul numérique des écoulements des fluides de Bingham et des fluides newtoniens incompressibles par la méthode des éléments finis. Ph.D. thesis, Université Paris VI

Fortin M, Glowinski R (1983) Augmented Lagrangian methods. Elsevier

Fraggedakis D, Dimakopoulos Y, Tsamopoulos J (2016) Yielding the yield-stress analysis: a study focused on the effects of elasticity on the settling of a single spherical particle in simple yield-stress fluids. Soft Matter

Frigaard IA, Nouar C (2005) On the usage of viscosity regularisation methods for visco-plastic fluid flow computation. J Non-Newt Fluid Mech 127(1):1–26

Fuchs M, Grotowski JF, Reuling J (1996) On variational models for quasi-static Bingham fluids. Math Meth Appl Sci 19(12):991–1015

Fuchs M, Seregin G (1997) Some remarks on non-Newtonian fluids including nonconvex perturbations of the Bingham and Powell–Eyring model for viscoplastic fluids. Math Models Meth Appl Sci 7(03):405–433

Fuchs M, Seregin G (1998) Regularity results for the quasi–static Bingham variational inequality in dimensions two and three. Math Z 227(3):525–541

Fuchs M, Seregin G (2000) Variational methods for problems from plasticity theory and for generalized Newtonian fluids. Springer
Fullsack P (1995) An arbitrary Lagrangian-Eulerian formulation for creeping flows and its application in tectonic models. Geophys J Int 120(1):1–23
Glowinski R (1980) Lecture on numerical methods for nonlinear variational problems. Springer
Glowinski R, Le Tallec P (1989) Augmented Lagrangian and operator splitting methods in nonlinear mechanics. SIAM, Philadelphia, USA
Glowinski R, Lions JL, Trémolières R (1981) Numerical analysis of variational inequalities. Elsevier
Glowinski R, Wachs A (2011) On the numerical simulation of viscoplastic fluid flow. In: Ciarlet PG, Lions JL (eds) Handbook of numerical analysis. Volume 16. Numerical methods for non-Newtonian fluids, chap. 6. Elsevier, pp 483–717
Goddard JD (1984) Dissipative materials as models of thixotropy and plasticity. J Non-Newt Fluid Mech 14:141–160
Gordon RJ, Schowalter WR (1972) Anisotropic fluid theory: a different approach to the dumbbell theory of dilute polymer solutions. J Rheol 16:79–97
Gray JMNT, Edwards AN (2014) A depth-averaged $\mu(I)$ rheology for shallow granular free-surface flows. J Fluid Mech 755:503–534
Grinevich PP, Olshanskii MA (2009) An iterative method for the Stokes type problem with variable viscosity. SIAM J Sci Comp 31(5):3959–3978
Henaut I, Brucy F (2001) Description rhéologique des bruts paraffiniques gélifies. In: Congrès du groupe Francais de rhéologie
Herschel WH, Bulkley T (1926) Measurement of consistency as applied to rubber-benzene solutions. Proc Amer Soc Testg Mater 26(2):621–633
Hestenes MR (1969) Multiplier and gradient methods. J Optim Theory Appl 4(5):303–320
Hirt CW, Nichols BD (1981) Volume of fluid (VOF) method for the dynamics of free boundaries. J Comput Phys 39(1):201–225
Hormozi S, Wielage-Burchard K, Frigaard IA (2011) Multi-layer channel flows with yield stress fluids. J Non-Newt Fluid Mech 166(5):262–278
Houska M (1981). Engineering aspects of the rheology of thixotropic liquids. Ph.D thesis, Faculty of Mechanical Engineering, Czech Techincal University of Prague
Huilgol RR, Kefayati GHR (2015) Natural convection problem in a Bingham fluid using the operator-splitting method. J Non-Newt Fluid Mech 220:22–32
Hupper HE (1982) The propagation of two-dimensional and axisymmetric viscous gravity currents over a rigid horizontal surface. J Fluid Mech 121:43–58
Ionescu IR (2010) Onset and dynamic shallow flow of a viscoplastic fluid on a plane slope. J Non-Newt Fluid Mech 165(19):1328–1341
Ionescu IR (2013) Augmented Lagrangian for shallow viscoplastic flow with topography. J Comput Phys 242:544–560
Ionescu IR, Lupaşcu O (2015) Modeling shallow avalanche onset over complex basal topography. Adv Comput Math:1–22
Ionescu IR, Mangeney A, Bouchut F, Roche O (2015) Viscoplastic modelling of granular column collapse with pressure and rate dependent viscosity. J Non-Newt Fluid Mech 219:1–18
Jop P, Forterre Y, Pouliquen O (2006) A constitutive law for dense granular flows. Nature 441:727–730
Karimfazli I, Frigaard IA, Wachs A (2015) A novel heat transfer switch using the yield stress. J Fluid Mech 783:526–566
Karimfazli I, Frigaard IA, Wachs A (2016) Thermal plumes in viscoplastic fluids: flow onset and development. J Fluid Mech 787:474–507
Ladd AJC, Verberg R (2001) Lattice-Boltzmann simulations of particle-fluid suspensions. J Stat Phys 104(5):1191–1251
Lagrée PY, Staron L, Popinet S (2011) The granular column collapse as a continuum: validity of a two-dimensional Navier–Stokes model with a $\mu(I)$-rheology. J Fluid Mech 686:378–408
Laigle D, Coussot P (1997) Numerical modeling of mudflows. J Hydr Engrg 123(7):617–623
Latché JC, Vola D (2005) Analysis of the Brezzi-Pitkäranta stabilized Galerkin scheme for creeping flows of Bingham fluids. SIAM J Numer Anal 42(3):1208–1225
Liu KF, Mei CC (1990) Approximation equations for the slow spreading of a thin Bingham plastic fluid. Phys Fluids A 2(1):30–36
Liu Y, Balmforth NJ, Hormozi S, Hewitt DR (2016) Two–dimensional viscoplastic dambreaks. J Non-Newt Fluid Mech in press
Maleki A, Hormozi S, Roustaei A, Frigaard IA (2015) Macro-size drop encapsulation. J Fluid Mech 769:482–521
Midi G (2004) On dense granular flows. Eur Phys J E 14(4):341–365
Mitsoulis E, Abdali SS, Markatos NC (1993) Flow simulation of Herschel-Bulkley fluids through extrusion dies. Can J Chem Engrg 71:147–160
Mitsoulis E, Huilgol RR (2004) Entry flows of Bingham plastics in expansions. J Non-Newt Fluid Mech 122:45–54
Mitsoulis E, Tsamopoulos J (2016) Numerical simulation of complex yield stress fluid flows. Rheol Acta submitted
Mittal R, Iaccarino G (2005) Immersed boundary methods. Annu Rev Fluid Mech 37:239–261
Moore F (1959) The rheology of ceramic slips and bodies. Trans Br Ceram Soc 58:470–494
Mosolov PP, Miasnikov VP (1965) Variational methods in the theory of the fluidity of a viscous-plastic medium. J Appl Math Mech 29(3):545–577
Mosolov PP, Miasnikov VP (1966) On stagnant flow regions of a viscous-plastic medium in pipes. J Appl Math Mech 30(4):841–853
Mosolov PP, Miasnikov VP (1967) On qualitative singularities of the flow of a viscoplastic medium in pipes. J Appl Math Mech 31(3):609–613
Moyers-Gonzalez MA, Frigaard IA (2004) Numerical solution of duct flows of multiple visco-plastic fluids. J Non-Newt Fluid Mech 127:227–241
Mujumdar A, Beris AN, Metzner AB (2002) Transient phenomena in thixotropic systems. J Non-Newt Fluid Mech 102:157–178
Muravleva E, Olshanskii MA (2008) Two finite-difference schemes for calculation of Bingham fluid flows in a cavity. Russ J Numer Anal Math Modell 23(6):615–634
Muravleva L (2015) Uzawa-like methods for numerical modeling of unsteady viscoplastic Bingham medium flows. Appl Numer Math 93:140–149
Muravleva L, Muravleva E, Georgiou GC, Mitsoulis E (2010) Numerical simulations of cessation flows of a Bingham plastic with the augmented Lagrangian method. J Non-Newt Fluid Mech 165:544–550
Negrão COR, Franco AT, Rocha LLV (2011) A weakly compressible flow model for the restart of thixotropic drilling fluids. J Non-Newt Fluid Mech 166(23):1369–1381
Nikitin KD, Olshanskii MA, Terekhov KM, Vassilevski YV (2011) Numerical method for the simulation of free surface flows of viscoplastic fluid in 3D. J Comput Math 29:605–622
Nirmalkar N, Bose A, Chhabra RP (2014) Free convection from a heated circular cylinder in Bingham plastic fluids. Int J Thermal Sci 83:33–44
Nirmalkar N, Chhabra RP, Poole RJ (2013) Laminar forced convection heat transfer from a heated square cylinder in a Bingham plastic fluid. Int J Heat Mass Transf 56(1):625–639

Oldroyd JG (1947) A rational formulation of the equations of plastic flow for a Bingham fluid. Proc Camb Philos Soc 43:100–105

Oldroyd JG (1950) On the formulation of rheological equations of states. Proc R Soc Lond A 200:523–541

Olshanskii MA (2009) Analysis of semi-staggered finite-difference method with application to Bingham flows. Comput Meth Appl Mech Engrg 198:975–985

Ovarlez G, Barral Q, Coussot P (2010) Three-dimensional jamming and flows of soft glassy materials. Nat Mat 9:115–119

Papanastasiou TC (1987) Flow of materials with yield. J Rheol 31:385–404

Park YS, Liu PLF (2010) Oscillatory pipe flows of a yield-stress fluid. J Fluid Mech 658:211–228

Powell MJD (1969) A method for nonlinear constraints in minimization problems. pages 283–298. Academic Press, London

Prashant DerksenJJ (2011) Direct simulations of spherical particle motion in Bingham liquids. Comput Chem Engrg 35(7):1200–1214

Putz A, Frigaard IA (2010) Creeping flow around particle in a Bingham fluid. J Non-Newt Fluid Mech 165(5–6):263–280

Putz A, Frigaard IA, Martinez DM (2009) On the lubrication paradox and the use of regularisation methods for lubrication flows. J Non-Newt Fluid Mech 163:62–77

Rickenmann D, Laigle D, McArdell BW, Hübl J (2006) Comparison of 2D debris-flow simulation models with field events. Comput Geo 10(2):241–264

Rockafellar RT (1976) Augmented Lagrangians and applications of the proximal point algorithm in convex programming. Math Oper Res 1(2):97–116

Roquet N, Saramito P (2003) An adaptive finite element method for Bingham fluid flows around a cylinder. Comput Meth Appl Mech Engrg 192(31-32):3317–3341

Roquet N, Saramito P (2008) An adaptive finite element method for viscoplastic flows in a square pipe with stick-slip at the wall. J Non-Newt Fluid Mech 155:101–115

Roustaei A, Frigaard IA (2013) The occurrence of fouling layers in the flow of a yield stress fluid along a wavy-walled channel. J Non-Newt Fluid Mech 198:109–124

Roustaei A, Gosselin A, Frigaard IA (2015) Residual drilling mud during conditioning of uneven boreholes in primary cementing. Part 1: rheology and geometry effects in non-inertial flows. J Non-Newt Fluid Mech 220:87–98

Barré de Saint-Venant AJC (1871) Théorie et équations générales du mouvement non permanent des eaux courantes. C R Acad Sci Paris 73:147–154

Saramito P (1994) Numerical simulation of viscoelastic fluid flows using incompressible finite element method and a θ-method. Math Model Numer Anal 28(1):1–35

Saramito P (2007) A new constitutive equation for elastoviscoplastic fluid flows. J Non-Newt Fluid Mech 145(1):1–14

Saramito P (2009) A new elastoviscoplastic model based on the Herschel-Bulkley viscoplasticity. J Non-Newt Fluid Mech 158(1–3):154–161

Saramito P (2016a) Complex fluids: modelling and algorithms. Springer

Saramito P (2016b) A damped Newton algorithm for computing viscoplastic fluid flows. J Non-Newt Fluid Mech in press. https://hal.archives-ouvertes.fr/hal-01228347/document

Saramito P, Roquet N (2001) An adaptive finite element method for viscoplastic fluid flows in pipes. Comput Meth Appl Mech Engrg 190(40-41):5391–5412

Savage SB (1984) The mechanics of rapid granular flows. Adv Appl Mech 24:289–366

Savage SB, Hutter K (1989) The motion of a finite mass of granular material down a rough incline. J Fluid Mech 199:177–215

Schechter RS, Wissler EH (1959) Heat transfer to Bingham plastics in laminar flow through circular tubes with internal heat generation. Nuclear Sci Engrg 6(5):371–375

Schwedoff T (1900) La rigidité des liquides. Congrès Int Phys, Paris 1:478–486

Sestak J, Charles ME, Cawkwell MG, Houska M (1987) Start-up of gelled crude oil pipelines. J Pipelines 6(1):15–24

Singh JP, Denn MM (2008) Interacting two-dimensional bubbles and droplets in a yield-stress fluid. Phys Fluids 20(4):040901

Smyrnaios DN, Tsamopoulos J (2001) Squeeze flow of Bingham plastics. J Non-Newt Fluid Mech 100(1):165–189

Sussman M, Smereka P, Osher S (1994) A level set approach for computing solutions to incompressible two-phase flow. J Comput Phys 114:146–159

Syrakos A, Georgiou GC, Alexandrou AN (2014) Performance of the finite volume method in solving regularised Bingham flows: inertia effects in the lid-driven cavity flow. J Non-Newt Fluid Mech 208:88–107

Szabo P, Hassager O (1992) Flow of viscoplastic fluids in eccentric annular geometries. J Non-Newt Fluid Mech 45(2):149–169

Szabo P, Hassager O (1997) Displacement of one Newtonian fluid by another: density effects in axial annular flow. Int J Multiphase Flow 23(1):113–129

Tanner RI, Walters K (1998) Rheology: an historical perspective. Elsevier

Tokpavi DL, Magnin A, Jay P (2008) Very slow flow of Bingham viscoplastic fluid around a circular cylinder. J Non-Newt Fluid Mech 154(1):65–76

Treskatis T, Moyers-Gonzalez MA, Price CJ (2015) A trust-region SQP method for the numerical approximation of viscoplastic fluid flow. submitted http://arxiv.org/pdf/1504.08057.pdf

Treskatis T, Moyers-Gonzalez MA, Price CJ (2016) An accelerated dual proximal gradient method for applications in viscoplasticity. J Non-Newt Fluid Mech in press

Tripathi MK, Sahu KC, Karapetsas G, Matar OK (2015) Bubble rise dynamics in a viscoplastic material. J Non-Newt Fluid Mech 222:217–226

Tsamopoulos J, Dimakopoulos Y, Chatzidai N, Karapetsas G, Pavlidis M (2008) Steady bubble rise and deformation in Newtonian and viscoplastic fluids and conditions for bubble entrapment. J Fluid Mech 601:123–164

Turan O, Chakraborty N, Poole RJ (2010) Laminar natural convection of Bingham fluids in a square enclosure with differentially heated side walls. J Non-Newt Fluid Mech 165(15):901–913

Turan O, Poole RJ, Chakraborty N (2011) Aspect ratio effects in laminar natural convection of Bingham fluids in rectangular enclosures with differentially heated side walls. J Non-Newt Fluid Mech 166(3):208–230

Unverdi SO, Tryggvason G (1992) A front-tracking method for viscous, incompressible, multi-fluid flows. J Comput Phys 100(1):25–37

Vikhansky A (2009) Thermal convection of a viscoplastic liquid with high Rayleigh and Bingham numbers. Phys Fluids 21(10): 103103

Vikhansky A (2010) On the onset of natural convection of Bingham liquid in rectangular enclosures. J Non-Newt Fluid Mech 165(23):1713–1716

Vikhansky A (2011) On the stopping of thermal convection in viscoplastic liquid. Rheol Acta 50(4):423–428

Vinay G, Wachs A, Agassant JF (2005) Numerical simulation of non-isothermal viscoplastic waxy crude oil flows. J Non-Newt Fluid Mech 128(2):144–162

Vola D, Babik F, Latché JC (2004) On a numerical strategy to compute gravity currents of non-Newtonian fluids. J Comput Phys 201(2):397–420

Vola D, Boscardin L, Latché JC (2003) Laminar unsteady flows of Bingham fluids: a numerical strategy and some benchmark results. J Comput Phys 187:441–456
Wachs A (2007) Numerical simulation of steady Bingham flow through an eccentric annular cross-section by distributed Lagrange multiplier/fictitious domain and augmented Lagrangian methods. J Non-Newt Fluid Mech 142:183–198
Wachs A, Frigaard IA (2016). Particle settling in yield stress fluids: limiting time, distance and applications. J Non-Newt Fluid Mech in press
Wachs A, Vinay G, Frigaard IA (2009) A 1.5D numerical model for the start up of weakly compressible flow of a viscoplastic and thixotropic fluid in pipelines. J Non-Newt Fluid Mech 159(1):81–94
Wilson SDR, Taylor AJ (1996) The channel entry problem for a yield stress fluid. J Non-Newt Fluid Mech 65:165–176
Yang WJ, Yeh HC (1965) Free convective flow of Bingham plastic between two vertical plates. J Heat Transf 87(2):319–320
Yu Z, Wachs A (2007) A fictitious domain method for dynamic simulation of particle sedimentation in Bingham fluids. J Non-Newt Fluid Mech 145:78–91
Zhang J (2010) An augmented Lagrangian approach to Bingham fluid flows in a lid-driven square cavity with piecewise linear equal-order finite elements. Comput Meth Appl Mech Engrg 199:3051–3057
Zhang J, Vola D, Frigaard IA (2006) Yield stress effects on Rayleigh-Bénard convection. J Fluid Mech 566:389–420
Zhang Y (2003) Error estimates for the numerical approximation of time-dependent flow of Bingham fluid in cylindrical pipes by the regularization method. Numer Math 96:153–184
Zisis T, Mitsoulis E (2002) Viscoplastic flow around a cylinder kept between parallel plates. J Non-Newt Fluid Mech 105:1–20